ESAIM: M2AN 58 (2024) 927–955
https://doi.org/10.1051/m2an/2024027

ESAIM: Mathematical Modelling and Numerical Analysis
www.esaim-m2an.org

NEW PIPE ELEMENT BASED ON HERMITE-JACKSON INTERPOLATION

Eliass Zafati[1,*] and Khuong Le Nguyen[2,3]

Abstract. A new pipe finite element is proposed for piping analysis within the framework of linear shell theory. The approach involves the use of a mixed interpolation of classical polynomial and trigonometric polynomial spaces, with trigonometric interpolation performed *via* Hermite-Jackson polynomials along the mid-surface section. Error estimates are provided and a convergence analysis is performed under specific assumptions on the regularity of the solution. The proposed element is validated through several numerical examples, which demonstrate its accuracy and efficiency in terms of computational cost. This method represents a promising approach for addressing the challenges of piping analysis.

Mathematics Subject Classification. 74K25, 42A15, 35J15, 74S05.

Received January 17, 2023. Accepted April 8, 2024.

1. Introduction

There has been a significant interest in the development of pipe-elbow finite element models for the analysis of the structural integrity of pipelines in various industries, such as oil and gas, nuclear power, and chemical processing. In engineering practices, the analysis of piping systems often involves studying complex networks with many pipes and complex loads, which can be computationally expensive when using three-dimensional shell elements. To address this issue, several simple pipe finite elements have been developed [2–4, 12, 15, 17, 19] that can capture the behavior of pipes and elbows under various loading and boundary conditions while minimizing computational costs and optimizing piping systems. One challenge in developing these models is accounting for the ovalization of the pipe cross-section which affect the structural integrity of the pipe and its ability to withstand these loads. Many of these models use a hybrid space approximation that combines polynomial spaces and Fourier sums, with the unknowns being the displacement, rotations, and Fourier coefficients. The use of Fourier sums is motivated by the periodic nature of the kinematic quantities over the contour of each section, which can be approximated using the Fourier partial sums where the resulting Fourier coefficients are known as the ovalization displacements. Moreover, to the best of the authors' knowledge, the literature lacks deep investigations on the error estimates associated with this kind of finite elements.

In this paper, a new pipe finite element has been developed and is fully described in curvilinear coordinates. As the existing Fourier-based pipe elements, the proposed element is capable of capturing the ovalization effect

Keywords and phrases. Linear shell theory, finite element method, Jackson polynomials, hermite trigonometric interpolation, error estimates.

[1] EDF R&D ERMES, 7 boulevard Gaspard Monge, 91120 Palaiseau, France.
[2] Faculty of Arts and Design, University of Canberra, Bruce 2617, Australia.
[3] Department of Civil Engineering, University of Transport Technology, Hanoi 100000, Vietnam.
*Corresponding author: eliass.zafati@edf.fr

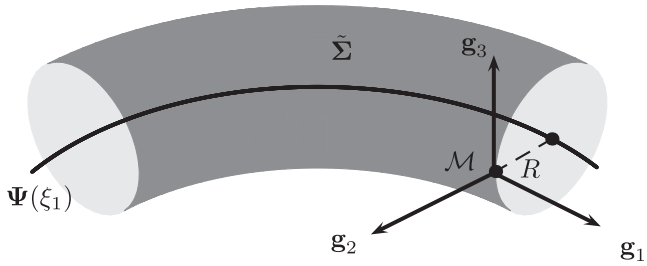

FIGURE 1. The mid-line Ψ and the covariant basis $(\mathbf{g})_i$ associated with a point $\mathcal{M}$ located at the mid-surface $\tilde{\Sigma}$.

that occurs in pipes under internal pressure or bending loads. More specifically, it is based on a combination of traditional polynomial interpolation, commonly used in beam and bar elements, and Hermite-Jackson trigonometric interpolation [11], which is constructed using Féjer kernels and associated polynomials of the second kind. Compared to existing piping elements, the present element has two main distinctive features:

- The unknowns, or the degrees of freedom, associated with the new element are explicitly the displacements and rotations at the discretization nodes, rather than Fourier coefficients. This allows the new element to be similar to standard finite elements, without the need for intermediate steps to compute Fourier sums or Fourier coefficients associated with the kinematic quantities or the boundary conditions. Moreover, the present element can be easily integrated into existing algorithms that deal with coupling problems in solid mechanics [8,16,18] or multi-physics problems, such as fluid-structure interaction (FSI) problems, where the constraints between different finite elements are typically expressed in terms of displacements and velocities. Using the same kind of degrees of freedom as shell elements, it simplifies the process of connecting the present element to shell elements unlike the Fourier-based pipe elements.
- The integral approximations are based on a combination of the quadratic Gauss and a closed type Gauss-Chebyshev formulas, in contrast to existing elements which are mainly based on a combination of the quadratic Gauss and Simpson formulas. The use of the closed-type Gauss-Chebyshev formula is solely motivated by its capability to achieve exact integration for trigonometric polynomials with the appropriate number of integration points. However, assessing the impact on the global accuracy of the two aforementioned integration rules is beyond the scope of this paper.

This paper is organized as follows: The subsequent section provides a brief overview of shell equations for curved pipes within the framework of linear elasticity. Section 3 introduces the new pipe element and provides a detailed description of the formulation. The numerical discretization strategy and convergence analysis are discussed in Section 4. Finally, the last section presents numerical examples for validation purposes.

2. Linear shell theory for pipes

This section provides a brief review of the elastic shell equations for pipes and the kinematic and geometric assumptions used in this paper. For a more detailed review of the mathematical aspects of general shell theory, the reader is referred to the reference [6].

We consider a pipe whose mid-surface is described by a compact domain $\tilde{\Sigma} \subset \mathbb{R}^3$, with a constant radius R and thickness e (as shown in Fig. 1), where $e \ll R$. The mid-line of the pipe, or the set of centroids of the cross sections of the pipe, is described by a smooth curve $\Psi : [0, L] \to \mathbb{R}^3$, where the position of the centroids is determined by the arc length ξ_1. At each point on the curve Ψ, the tangent vector $\mathbf{e}_{\xi_1}$ is defined as:

$$\mathbf{e}_{\xi_1} = \Psi'(\xi_1). \tag{2.1}$$

For sake of simplicity, we assume that the tangent vector $\mathbf{e}_{\xi_1}$ is unit. The curvature $\kappa(\xi_1) \geq 0$ is given by:

$$\Psi''(\xi_1) = \kappa(\xi_1)\mathbf{n}. \tag{2.2}$$

In the following, the unit vector $\mathbf{b}$ is defined as the cross product of $\mathbf{e}_{\xi_1}$ and $\mathbf{n}$, *i.e.*, $\mathbf{b} = \mathbf{e}_{\xi_1} \times \mathbf{n}$. It is assumed that $\mathbf{b}$ is constant, which means that the torsion vanishes and the mid-line Ψ stays in the same plane. Therefore, we can conclude that:

$$\frac{d\mathbf{n}}{d\xi_1} = -\kappa(\xi_1)\mathbf{e}_{\xi_1}. \tag{2.3}$$

Now, we define the frame $(\mathbf{e}_{\xi_2}, \mathbf{e}_{\xi_3})$ associated with each pipe cross section by:

$$\mathbf{e}_{\xi_2} = -\sin\left(\tfrac{\xi_2}{R}\right)\mathbf{n} + \cos\left(\tfrac{\xi_2}{R}\right)\mathbf{b} \quad \text{and} \quad \mathbf{e}_{\xi_3} = \cos\left(\tfrac{\xi_2}{R}\right)\mathbf{n} + \sin\left(\tfrac{\xi_2}{R}\right)\mathbf{b} \quad \text{and} \quad \xi_2 \in [0, 2\pi R]. \tag{2.4}$$

Given the definitions in (2.7) and (2.2), it is easy to see that the domain $\hat{\Omega}$ describing the pipe volume is the image of the following map $\Theta : \bar{\Omega} = [0, L] \times [0, 2\pi R] \times [-\frac{e}{2}, \frac{e}{2}] \to \mathbb{R}^3$ (Ω is the interior of $\bar{\Omega}$):

$$\Theta(\xi_1, \xi_2, \xi_3) = \Psi(\xi_1) + (R + \xi_3)\mathbf{e}_{\xi_3}. \tag{2.5}$$

It is seen that the mid-surface in the reference configuration coincides with $\Theta^{-1}(\tilde{\Sigma}) = [0, L] \times [0, 2\pi R] \times \{0\}$. The covariant basis $(\mathbf{g}_i)_{1\leq i\leq 3}$ at each point of $\hat{\Omega}$ (or the basis of the tangent space) is computed through the formula:

$$\mathbf{g}_i = \frac{\partial \Theta}{\partial \xi_i}. \tag{2.6}$$

Using (2.5), the components of $\mathbf{g}_i$ ($i \in \{1, 2, 3\}$) in the basis $(\mathbf{e}_{\xi_i})_{1\leq i\leq 3}$ are:

$$\mathbf{g}_1 = \begin{pmatrix} 1 - \kappa(R + \xi_3)\cos(\frac{\xi_2}{R}) \\ 0 \\ 0 \end{pmatrix} \quad \mathbf{g}_2 = \begin{pmatrix} 0 \\ \frac{\xi_3 + R}{R} \\ 0 \end{pmatrix} \quad \mathbf{g}_3 = \begin{pmatrix} 0 \\ 0 \\ 1 \end{pmatrix}. \tag{2.7}$$

It is seen that $(\mathbf{g}_i)_{1\leq i\leq 3}$ is a basis if and only if $\max\limits_{\xi_1\in[0,L]} \kappa(\xi_1)(R + \frac{e}{2}) < 1$, which also means that Θ is a local diffeomorphism on Ω if the radius of the curvature remains greater than the radius $R + \frac{e}{2}$. Henceforth, we assume the following:

(**Hr**): $\max\limits_{\xi_1\in[0,L]} \kappa(\xi_1)\left(R + \frac{e}{2}\right) < 1$.

In the context of shell kinematics, the displacement field at each point $(\xi_1, \xi_2, \xi_3) \in \bar{\Omega}$ of the material is expressed as:

$$\mathbf{U}(\xi_1, \xi_2, \xi_3) = \mathbf{u}(\xi_1, \xi_2) + \xi_3\left(\theta_1(\xi_1, \xi_2)\,\tilde{\mathbf{e}}_{\xi_1} + \theta_2(\xi_1, \xi_2)\,\tilde{\mathbf{e}}_{\xi_2}\right) \tag{2.8}$$

where $(\tilde{\mathbf{e}}_{\xi_i})_{1\leq i\leq 3}$ is the contravariant basis of $(\mathbf{e}_{\xi_i})_{1\leq i\leq 3}$. The kinematical assumption in (2.8) is called the Reissner-Mindlin kinematical assumption. The second term on the right side of equation (2.8) accounts for the displacement resulting from the rotation of the line perpendicular to the mid-surface in the initial configuration (prior to deformation). The linearized strains in curvilinear coordinates can be expressed in terms of the displacement field $\mathbf{U}$ as follows:

$$e_{i\|j} = \frac{1}{2}\left(\frac{\partial \mathbf{U}}{\partial \xi_i} \cdot \mathbf{g}_j + \frac{\partial \mathbf{U}}{\partial \xi_j} \cdot \mathbf{g}_i\right) \tag{2.9}$$

where $(e_{i\|j})_{1\leq i,j\leq 3}$ is symmetric. Using (2.8), we get:

$$\begin{cases} e_{1\|1} = \left(1-\kappa(R+\xi_3)\cos\left(\frac{\xi_2}{R}\right)\right)\left[\frac{\partial \mathbf{u}}{\partial \xi_1}\cdot \mathbf{e}_{\xi_1} + \xi_3\frac{\partial \theta_1}{\partial \xi_1} + \xi_3\kappa\sin\left(\frac{\xi_2}{R}\right)\theta_2\right] \\ e_{2\|2} = \frac{R+\xi_3}{R}\left[\frac{\partial \mathbf{u}}{\partial \xi_2}\cdot \mathbf{e}_{\xi_2} + \xi_3\frac{\partial \theta_2}{\partial \xi_2}\right] \\ e_{3\|3} = 0 \\ 2e_{1\|2} = \left(1-\kappa(R+\xi_3)\cos\left(\frac{\xi_2}{R}\right)\right)\left[\frac{\partial \mathbf{u}}{\partial \xi_2}\cdot \mathbf{e}_{\xi_1} + \xi_3\frac{\partial \theta_1}{\partial \xi_2}\right] + \frac{R+\xi_3}{R}\left[\frac{\partial \mathbf{u}}{\partial \xi_1}\cdot \mathbf{e}_{\xi_2} + \xi_3\frac{\partial \theta_2}{\partial \xi_1} - \xi_3\kappa\sin\left(\frac{\xi_2}{R}\right)\theta_1\right] \\ 2e_{1\|3} = \left(1-\kappa R\cos\left(\frac{\xi_2}{R}\right)\right)\theta_1 + \frac{\partial \mathbf{u}}{\partial \xi_1}\cdot \mathbf{e}_{\xi_3} \\ 2e_{2\|3} = \theta_2 + \frac{\partial \mathbf{u}}{\partial \xi_2}\cdot \mathbf{e}_{\xi_3} \end{cases} \tag{2.10}$$

where the derivatives are assumed to be well-defined. In some references, the expression of $(e_{i\|j})_{1\leq i,j\leq 3}$ is written as a decomposition into membrane, bending and shear strain tensors. For sake of simplicity, the paper is focused on the membrane-bending model since the proposed finite element may be trivially adapted to the other shell models. In the subsequent, we assume:

$$e_{2\|3} = e_{1\|3} = 0. \tag{2.11}$$

In particular, we have:

$$\begin{cases} \theta_1 = \frac{1}{\left(1-\kappa R\cos\left(\frac{\xi_2}{R}\right)\right)}\left[-\kappa\cos\left(\frac{\xi_2}{R}\right)u_1 - \frac{\partial u_3}{\partial \xi_1}\right] \\ \theta_2 = \frac{1}{R}u_2 - \frac{\partial u_3}{\partial \xi_2} \end{cases} \tag{2.12}$$

where $(u_i)_{1\leq i\leq 3}$ are the components of $\mathbf{u}$ in the contravariant basis $(\tilde{\mathbf{e}}_{\xi_i})_{1\leq i\leq 3}$. Hence, the strain tensor $(e_{i\|j})_{1\leq i,j\leq 2}$ only depends on the vector field $\mathbf{u}$. In this case, the elasticity tensor $(\mathbf{A}^{ijkl})_{1\leq i,j,k,l\leq 2}$ for plane stress problems is adopted and is given by:

$$\mathbf{A}^{ijkl} = \frac{E}{2(1+\nu)}\left(g^{ik}g^{jl} + g^{il}g^{jk} + \frac{2\nu}{1-\nu}g^{ij}g^{kl}\right) \tag{2.13}$$

where E, ν stand for the Young modulus and Poisson ratio, respectively. The scalars $g^{ij} = \mathbf{g}^i\cdot\mathbf{g}^j$ are the components of the contravariant metric tensor. One may notice that the components g^{ij} are well-defined by the hypothesis (**Hr**) and we have, in addition, $g^{ij} = 0$ if $i \neq j$. Now, it is convenient to define the operator $\mathbf{T}$ mapping the vector $\mathbf{u}$ to the right hand side of (2.8), where θ_1 and θ_2 are expressed in terms of the filed $\mathbf{u}$ using the conditions (2.11).

Throughout this paper, we are concerned with the following variational problem $(\mathcal{P})$ which consists on finding $\mathbf{u}\in\mathbf{V}(\Sigma)$ such that:

$$\mathbf{a}(\mathbf{u},\mathbf{v}) = \int_\Omega \mathbf{A}^{ijkl}e_{i\|j}(\mathbf{u})e_{k\|l}(\mathbf{v})\sqrt{g}dx = \int_{\Gamma_1}\mathbf{h}\cdot\gamma\mathbf{T}\mathbf{v}\sqrt{g}\,d\Gamma \quad \forall\mathbf{v}\in\mathbf{V}(\Sigma) \tag{2.14}$$

where:

- $\Sigma = (0,L)\times(0,2\pi R)$
- $\Gamma_0,\Gamma_1\subset\partial\Omega\setminus\left[(0,L)\times\{0\}\times(-\frac{e}{2},\frac{e}{2})\cup(0,L)\times\{2\pi R\}\times(-\frac{e}{2},\frac{e}{2})\right]$ relatively open parts
- γ is the trace operator
- $(u_i)_{1\leq i\leq 3}$ are the components of $\mathbf{u}$ in the contravariant basis $(\tilde{\mathbf{e}}_{\xi_i})_{1\leq i\leq 3}$

– $\mathbf{h} \in \bigtimes_{i=1}^{3} \mathrm{H}^{-\frac{1}{2}}(\Gamma_1)$ represents the external load field with contravariant components

The Hilbert space $\mathbf{V}(\Sigma)$ is defined by:

$$\mathbf{V}(\Sigma) = \left\{\mathbf{u} = (u_i)_{1\leq i\leq 3} \in \mathrm{H}^1(\Sigma) \times \mathrm{H}^1(\Sigma) \times \mathrm{H}^2(\Sigma); \mathbf{T}\mathbf{u} = 0 \text{ on } \Gamma_0\right\} \tag{2.15}$$

and endowed with the norm:

$$\|\mathbf{u}\|_{\mathbf{V}(\Sigma)} = \sum_{i=1}^{2} \|u_i\|_{\mathrm{H}^1(\mathbf{\Sigma})} + \|u_3\|_{\mathrm{H}^2(\mathbf{\Sigma})}. \tag{2.16}$$

It is seen that $\mathbf{T}$ is continuous from $\mathbf{V}(\Sigma)$ to $\mathbf{T}(\mathbf{V}(\Sigma)) \subset \bigtimes_{i=1}^{3} \mathrm{H}^1(\Omega)$. Thus, the term $\gamma\mathbf{T}\mathbf{v}$ is well-defined as well as the right hand side of the probem (2.14). The well-posedness of the problem $(\mathcal{P})$ is a direct application of Lax-Milgram theorem using the following coercivity result:

Lemma 2.1. *There exists a constant $C > 0$ such that:*

$$\mathbf{a}(\mathbf{u}, \mathbf{u}) \geq C\|\mathbf{u}\|^2_{\mathbf{V}(\Sigma)} \quad \forall \mathbf{u} \in \mathbf{V}(\Sigma). \tag{2.17}$$

In particular, C depends on R and e.

Proof. The proof is only a consequence of Theorem 1.7–4 in [6] and an equivalence of norms argument (see for instance Proposition 4.3.2 in [5] for similar arguments). □

3. New pipe element and Jackson interpolation

The strategy for constructing the new finite element is based on the fact that the solution $\mathbf{u} \in \mathbf{V}(\Sigma)$ to the problem $(\mathcal{P})$ depends only on the curvilinear coordinates $0 \leq \xi_1 \leq L$ and $0 \leq \xi_2 \leq 2\pi R$, and is $2\pi R$-periodic with respect to ξ_2. The idea in the subsequent is to divided the mid surface $\bar{\Sigma} = [0, L] \times [0, 2\pi R]$ into several elements of the form $\mathbf{K} = [\xi_{1,0}, \xi_{1,1}] \times [0, 2\pi R]$, where $0 \leq \xi_{1,0}, \xi_{1,1} \leq L$. Hence, the resulting pipe element is two-dimensional and will be characterized by a combination of two different approximations: one with respect to the variable ξ_1 using classical polynomials and one with respect to the variable ξ_2 using Hermite-Jackson trigonometric polynomials. The set of polynomials of a single variable of degree less than or equal to k is denoted by $\mathbb{P}_k$ $(k \geq 1)$, and the set of 2π-periodic trigonometric polynomials of order less than or equal to n is denoted by $\mathbb{T}_n$.

Following the framework in [7], we first introduce the new finite element in the reference configuration with respect to the curvilinear coordinates $(\hat{\xi}_1, \hat{\xi}_2)$, refereed in this paper as the triple $\left(\hat{\mathbf{K}}, \mathbf{P}^{[k,N_2]}_{\hat{\mathbf{K}}}, \mathbf{T}^{\star}_{\hat{\mathbf{K}}}\right)$, and characterized by the following properties:

– The compact $\hat{\mathbf{K}}$ is the square $[0, 1] \times [0, 2\pi]$
– Let $\mathbf{I}_{\hat{\mathbf{K}}} = [\![0, k]\!] \times [\![0, N_2]\!]$ with $k, N_2 > 0$ positive integers (recall that $[\![a, b]\!]$ stands for the interval of integers between the intergers a and b). We define the function space $\mathbf{P}^{[k,N_2]}_{\hat{\mathbf{K}}}$ of functions defined on $\hat{\mathbf{K}}$ as the set:

$$\mathbf{P}^{[k,N_2]}_{\hat{\mathbf{K}}} = \left\{\hat{p} \in \mathrm{span}\{\hat{p}_i \otimes \hat{t}_j, \hat{p}_i \otimes \hat{s}_j\}_{(i,j)\in\mathbf{I}_{\hat{\mathbf{K}}}} \mid \sum_{0\leq j\leq N_2} \frac{\partial \hat{p}}{\partial \hat{\xi}_2}(\hat{\xi}_1, \hat{\xi}_{2,j}) = 0\right\} \tag{3.1}$$

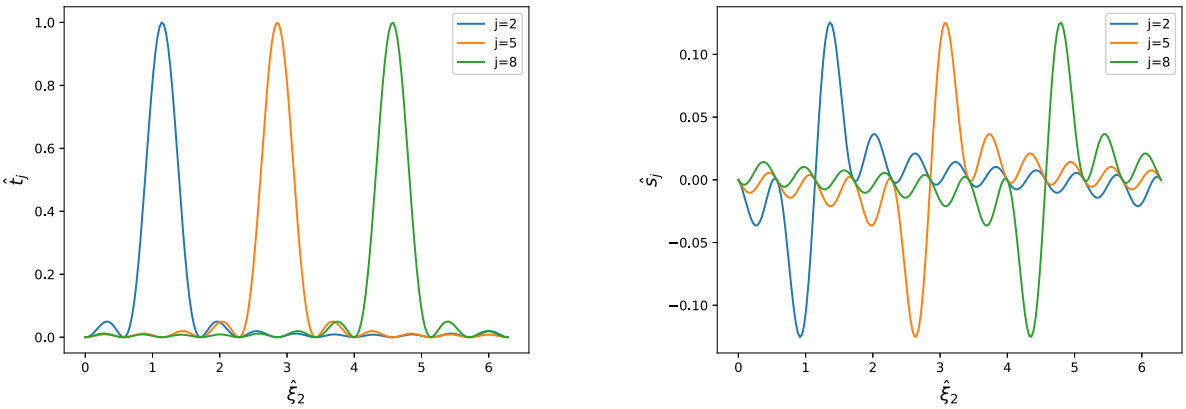

(a) (b)

FIGURE 2. Plots of the polynomials $\hat{t}_j$ (a) and $\hat{s}_j$ (b) for different values of j using $N_2 = 10$.

where the family $(\hat{p}_i)_{0\leq i\leq k}$ is a basis of the space $\mathbb{P}_k$. The trigonometric polynomials $\hat{t}_j$ and $\hat{s}_j$ in $\mathbb{T}_n$ are defined as follows:

$$\begin{cases} \hat{t}_j(\hat{\xi}_2) = \frac{1}{(N_2+1)^2}\left(\frac{\sin\frac{N_2+1}{2}(\hat{\xi}_2-\hat{\xi}_{2,j})}{\sin\frac{\hat{\xi}_2-\hat{\xi}_{2,j}}{2}}\right)^2 & 0\leq j\leq N_2 \\ \hat{s}_j(\hat{\xi}_2) = \frac{1}{(N_2+1)^2}\left\{1-\cos\left((N_2+1)\left(\hat{\xi}_2-\hat{\xi}_{2,j}\right)\right)\right\}\cot\frac{1}{2}\left(\hat{\xi}_2-\hat{\xi}_{2,j}\right) & 0\leq j\leq N_2 \\ \quad = \frac{2}{(N_2+1)^2}\sum_{l=1}^{N_2}\sin\left(l(\hat{\xi}_2-\hat{\xi}_{2,j})\right)+\frac{1}{(N_2+1)^2}\sin\left((N_2+1)(\hat{\xi}_2-\hat{\xi}_{2,j})\right) & \end{cases} \tag{3.2}$$

where the coordinates $\hat{\xi}_{2,j} = \frac{2\pi j}{N_2+1}$ for $0\leq j\leq N_2$ are the discrete points along the interval $[0, 2\pi]$ and , for every $(i,j)\in \mathbf{I}_{\hat{\mathbf{K}}}$, the multi-variable map $\hat{p}_i\otimes\hat{t}_j$ is defined on $\hat{\mathbf{K}}$ by $\hat{p}_i\otimes\hat{t}_j(\hat{\xi}_1,\hat{\xi}_2) = \hat{p}_i(\hat{\xi}_1)\hat{t}_j(\hat{\xi}_2)$ for every $(\hat{\xi}_1,\hat{\xi}_2)\in\mathbf{K}$. In the context of the finite element method, the maps $(\hat{p}_i\otimes\hat{t}_j)_{ij}$ and $(\hat{p}_i\otimes\hat{s}_j)_{ij}$ are commonly known as the basis functions. Moreover, the constraint condition defined in (3.1) is of particular interest since we have:

$$\mathbb{T}_{N_2} = \left\{\hat{p}\in \text{span}\{\hat{t}_0,\ldots,\hat{t}_{N_2},\hat{s}_0,\ldots,\hat{s}_{N_2},\}|\sum_{0\leq j\leq N_2}\frac{\partial\hat{p}}{\partial\hat{\xi}_2}(\hat{\xi}_1,\hat{\xi}_{2,j}) = 0\right\}. \tag{3.3}$$

Moreover, every trigonometric polynomial $\hat{t}\in\mathbb{T}_{N_2}$ is uniquely written as:

$$\hat{t} = \sum_{j=0}^{N_2}\hat{t}\left(\hat{\xi}_{2,j}\right)\,\hat{t}_j + \sum_{j=0}^{N_2}\hat{t}'\left(\hat{\xi}_{2,j}\right)\,\hat{s}_j. \tag{3.4}$$

Also, we have:

$$\begin{cases} \hat{t}_j(\hat{\xi}_{2,i}) = \delta_{ij} & \hat{t}'_j(\hat{\xi}_{2,j}) = 0 \\ \hat{s}_j(\hat{\xi}_{2,i}) = 0 & \hat{s}'_j(\hat{\xi}_{2,j}) = \delta_{ij}. \end{cases} \tag{3.5}$$

It is interesting to note that the the trigonometric polynomials $\hat{t}_j$ and $\hat{s}_j$ are directly related to the well-known Féjer and Conjugate Dirichlet kernels [9, 21]. Plots of the functions $\hat{s}_j$ and $\hat{t}_j$ for different values of j are depicted in Figure 2 using $N_2 = 10$. It is interesting to point out that the related discrete points $(\hat{\xi}_{2,j})_{0\leq j\leq N_2}$ are suitably chosen to satisfy interesting properties, stated in Lemma 3.3 below.

– The space $\mathbf{T}^{\star}_{\hat{\mathbf{K}}}$ is the finite set of linearly independent linear forms $\hat{\phi}_{ij}$ and $\hat{\psi}_{ij}$ defined on span$\{\hat{p}_i \otimes \hat{t}_j, \hat{p}_i \otimes \hat{s}_j\}_{(i,j)\in \mathbf{I}_{\hat{\mathbf{K}}}}$ such that :

$$\hat{p} = \sum_{(i,j)\in \mathbf{I}_{\hat{\mathbf{K}}}} \hat{\phi}_{ij}(\hat{p})\hat{p}_i \otimes \hat{t}_j + \sum_{(i,j)\in \mathbf{I}_{\hat{\mathbf{K}}}} \hat{\psi}_{ij}(\hat{p})\hat{p}_i \otimes \hat{s}_j \quad \forall \hat{p} \in \mathbf{P}^{[k,N_2]}_{\hat{\mathbf{K}}} \tag{3.6}$$

where:

$$\begin{cases} \hat{\phi}_{ij}(\hat{p}_k \otimes \hat{t}_l) = \delta_{ik}\delta_{jl} \quad \text{and} \quad \hat{\phi}_{ij}(\hat{p}_k \otimes \hat{s}_l) = 0 \quad \forall (i,j),(k,l) \in \mathbf{I}_{\hat{\mathbf{K}}} \\ \hat{\psi}_{ij}(\hat{p}_k \otimes \hat{s}_l) = \delta_{ik}\delta_{jl} \quad \text{and} \quad \hat{\psi}_{ij}(\hat{p}_k \otimes \hat{t}_l) = 0 \quad \forall (i,j),(k,l) \in \mathbf{I}_{\hat{\mathbf{K}}}. \end{cases} \tag{3.7}$$

In the context of the finite element method $\hat{\phi}_{ij}$ and $\hat{\psi}_{ij}$ are refereed as the degrees of freedom and represent the unknowns of the linear system generated by the discretized problem.

Now, for arbitrary compact $\mathbf{K}$ of the form $[\xi_{1,0}, \xi_{1,1}] \times [0, 2\pi R]$, with $\xi_{1,0} < \xi_{1,1}$, we define the finite element $\left(\mathbf{K}, \mathbf{P}^{[k,N_2]}_{\mathbf{K}}, \mathbf{T}^{\star}_{\mathbf{K}}\right)$ as follows: Let $\mathbf{F}_{\mathbf{K}} : \hat{\mathbf{K}} \to \mathbf{K}$ be the linear map defined by:

$$\mathbf{F}_{\mathbf{K}}(\hat{\xi}_1, \hat{\xi}_2) = \left((\xi_{1,1} - \xi_{1,0})\hat{\xi}_1 + \xi_{1,0}, R\hat{\xi}_2\right). \tag{3.8}$$

The space $\mathbf{P}^{[k,N_2]}_{\mathbf{K}}$ is given by:

$$\mathbf{P}^{[k,N_2]}_{\mathbf{K}} = \left\{ p = \hat{p} \circ \mathbf{F}^{-1}_{\mathbf{K}} \quad \text{with} \quad \hat{p} \in \mathbf{P}^{[k,N_2]}_{\hat{\mathbf{K}}} \right\} \tag{3.9}$$

with,

$$\begin{cases} t_j(.) &= \hat{t}_j\left(\frac{\cdot}{R}\right) \\ s_j(.) &= \hat{s}_j\left(\frac{\cdot}{R}\right) \\ p_i(.) &= \hat{p}_i\left(\frac{\cdot - \xi_{1,0}}{\xi_{1,1} - \xi_{1,0}}\right) \\ \xi_{2,j} &= R\hat{\xi}_{2,j}. \end{cases} \tag{3.10}$$

Thus, for every $(i,j) \in \mathbf{I}_{\hat{\mathbf{K}}}$, it is not difficult to establish that:

$$\begin{aligned} p_i \otimes t_j &= \hat{p}_i \otimes \hat{t}_j \circ \mathbf{F}^{-1}_{\mathbf{K}} \\ p_i \otimes s_j &= \hat{p}_i \otimes \hat{s}_j \circ \mathbf{F}^{-1}_{\mathbf{K}}. \end{aligned} \tag{3.11}$$

Finally, the space $\mathbf{T}^{\star}_{\mathbf{K}}$ is the set of linearly independent linear forms ϕ_{ij} and ψ_{ij} satisfying:

$$\begin{cases} \phi_{ij}(p_k \otimes t_l) = \delta_{ik}\delta_{jl} \quad \text{and} \quad \phi_{ij}(p_k \otimes s_l) = 0 \quad \forall (i,j),(k,l) \in \mathbf{I}_{\hat{\mathbf{K}}} \\ \psi_{ij}(p_k \otimes s_l) = \delta_{ik}\delta_{jl} \quad \text{and} \quad \psi_{ij}(p_k \otimes t_l) = 0 \quad \forall (i,j),(k,l) \in \mathbf{I}_{\hat{\mathbf{K}}}. \end{cases} \tag{3.12}$$

In this case, for every $p \in \mathbf{P}^{[k,N_2]}_{\hat{\mathbf{K}}}$, it is clear that:

$$p = \sum_{(i,j)\in \mathbf{I}_{\hat{\mathbf{K}}}} \phi_{ij}(p)p_i \otimes t_j + \sum_{(i,j)\in \mathbf{I}_{\hat{\mathbf{K}}}} \psi_{ij}(p)p_i \otimes s_j. \tag{3.13}$$

In particular, we have the following relationship between the linear forms for every $\hat{p} \in \mathbf{P}^{[k,N_2]}_{\hat{\mathbf{K}}}$:

$$\begin{cases} \hat{\phi}_{ij}(\hat{p}) = \phi_{ij}(p) \\ \hat{\psi}_{ij}(\hat{p}) = \psi_{ij}(p). \end{cases} \tag{3.14}$$

Remark 3.1. According to the definitions of $(\phi_{ij})_{ij}$ and $(\psi_{ij})_{ij}$, it is clear that if p is only an element of the span of the set $\{p_i \otimes t_j, p_i \otimes s_j\}_{(i,j)\in \mathbf{I}_{\hat{\mathbf{K}}}}$, then we can express it as:

$$p = \sum_{(i,j)\in \mathbf{I}_{\hat{\mathbf{K}}}} \phi_{ij}(p) p_i \otimes t_j + \sum_{(i,j)\in \mathbf{I}_{\hat{\mathbf{K}}}} \psi_{ij}(p) p_i \otimes s_j. \tag{3.15}$$

Example 3.2. If $\mathbb{P}_1$ is considered, we adopt the following linear forms:

$$\begin{cases} \phi_{ij}(p) = p\left(\xi_{1,i}, \xi_{2,j}\right) & \forall\, i = 0,1 \quad 0 \le j \le N_2 \\ \psi_{ij}(p) = \frac{\partial p}{\partial \xi_2}\left(\xi_{1,i}, \xi_{2,j}\right) & \forall\, i = 0,1 \quad 0 \le j \le N_2. \end{cases} \tag{3.16}$$

On the other hand, if $\mathbb{P}_3$ is considered, we take:

$$\begin{cases} \phi_{ij}(p) = p\left(\xi_{1,i}, \xi_{2,j}\right) & \forall\, 0 \le i \le 1 \quad 0 \le j \le N_2 \\ \phi_{ij}(p) = \frac{\partial p}{\partial \xi_1}\left(\xi_{1,i-2}, \xi_{2,j}\right) & \forall\, 2 \le i \le 3 \quad 0 \le j \le N_2 \\ \psi_{ij}(p) = \frac{\partial p}{\partial \xi_2}\left(\xi_{1,i}, \xi_{2,j}\right) & \forall\, 0 \le i \le 1 \quad 0 \le j \le N_2 \\ \psi_{ij}(p) = \frac{\partial^2 p}{\partial \xi_1 \partial \xi_2}\left(\xi_{1,i-2}, \xi_{2,j}\right) & \forall\, 2 \le i \le 3 \quad 0 \le j \le N_2. \end{cases} \tag{3.17}$$

It is seen that (3.16) and (3.17) both imply that the bases corresponding to the spaces $\mathbb{P}_1$ and $\mathbb{P}_3$ coincide with those, commonly, used for the bar and the beam finite elements, respectively. □

As the new finite element is introduced, the following Lemma summarizes some basic properties associated with $\left(\mathbf{K}, \mathbf{P}_{\mathbf{K}}^{[k,N_2]}, \mathbf{T}_{\mathbf{K}}^{\star}\right)$, useful in the sequel:

Lemma 3.3. *Given the definition of the finite element* $\left(\mathbf{K}, \mathbf{P}_{\mathbf{K}}^{[k,N_2]}, \mathbf{T}_{\mathbf{K}}^{\star}\right)$, *we claim:*

(1) The elements of the family $\{p_i \otimes t_j, p_i \otimes s_j\}_{(i,j)\in \mathbf{I}_{\hat{\mathbf{K}}}}$ *are linearly independent*

(2) Let $p \in \operatorname{span}\{p_i \otimes t_j, p_i \otimes s_j\}_{(i,j)\in \mathbf{I}_{\hat{\mathbf{K}}}}$, *then:*

$$p \in \mathbf{P}_{\mathbf{K}}^{[k,N_2]} \Longleftrightarrow \sum_{j=0}^{N_2} \psi_{ij}(p) = 0 \quad \forall i. \tag{3.18}$$

In particular, the dimension of the space $\mathbf{P}_{\mathbf{K}}^{[k,N_2]}$ *is* $(k+1)(2N_2+1)$

(3) Let $p \in \operatorname{span}\{p_i \otimes t_j, p_i \otimes s_j\}_{(i,j)\in \mathbf{I}_{\hat{\mathbf{K}}}}$, *for every* $0 \le j \le N_2$, *we have:*

$$\begin{cases} p(., \xi_{2,j}) & = \sum_{i=0}^{k} \phi_{ij}(p) p_i \\ \frac{\partial p}{\partial \xi_2}\left(., \xi_{2,j}\right) & = \sum_{i=0}^{k} \psi_{ij}(p) p_i. \end{cases} \tag{3.19}$$

(4) For every trigonometric polynomial $\hat{T} \in \mathbb{T}_{N_2}$, *we have:*

$$\int_0^{2\pi} \hat{T}\left(\hat{\xi}\right) d\hat{\xi} = \frac{2\pi}{N_2+1} \sum_{j=0}^{N_2} \hat{T}\left(\hat{\xi}_{2,j}\right). \tag{3.20}$$

In particular, we have:

$$\sum_{j=0}^{N_2} \hat{t}_j(\hat{\xi}_2) = 1 \quad \forall\, 0 \le \hat{\xi}_2 \le 2\pi. \tag{3.21}$$

(5) For every trigonometric polynomials $\hat{T}, \hat{S} \in \mathbb{T}_{N_2}$, we have:

$$\int_0^{2\pi} \hat{T}\left(\hat{\xi}\right) S\left(\hat{\xi}\right) d\hat{\xi} = \frac{2\pi}{N+1} \sum_{j=0}^{N} \hat{T}\left(\hat{\xi}_j\right) \hat{S}\left(\hat{\xi}_j\right) \tag{3.22}$$

for every integer $N \geq 2N_2$ and the vector $(\hat{\xi}_j)_{0\leq j\leq N}$ is such that $\hat{\xi}_j = \frac{2\pi j}{N+1}$.

Proof. The two first claims are simple to prove. The proof of the third claim is based on the identities (3.5). For the proof of (3.20) and (3.22), the reader may refer to [21]. The formula (3.21) can be deduced as follow: Indeed, we have $\hat{t}_j = \frac{2}{N_2+1} K_{N_2}(. - \hat{\xi}_{2,j})$, where K_{N_2} stands for the Fejr kernel, (see (3.2) chapter III in [21]), and combining (3.20) and the fact that $\frac{1}{\pi}\int_0^{2\pi} K_{N_2}(\hat{\xi}_2 - s)\, ds = 1$, we obtain the desired result. □

The last property in Lemma 3.3, referred in this paper as a closed type Gauss-Tchebychev integration, is particularly useful and will be combined with the Gauss quadrature rule to approximate the integrals over each finite element. In the numerical examples, we will focus on polynomial spaces of lower orders, $\mathbb{P}_1$ and $\mathbb{P}_3$, for simplicity. However, the convergence of the method will be analyzed in a general framework and under specific assumptions about the regularity of the solution.

Before introducing the definition of the local interpolant related to the present finite element, we first extend the definition of the linear forms ϕ_{ij} and ψ_{ij} to a larger space of smooth functions as follows: Let $(p_i^\star)_{0\leq i\leq k}$ denotes the biorthogonal functionals of $(p_i)_{0\leq i\leq k}$, *i.e.*, $p_i^\star(p_j) = \delta_{ij}\ \forall\, 0 \leq i, j \leq k$, it is not difficult to see that:

$$\begin{cases} p_i^\star(p(., \xi_{2,j})) & = \phi_{ij}(p) \\ p_i^\star(\frac{\partial p}{\partial \xi_2}(., \xi_{2,j})) & = \psi_{ij}(p) \end{cases} \tag{3.23}$$

for every $p \in \text{span}\{p_i \otimes t_j, p_i \otimes s_j\}_{(i,j)}$. It is seen that that every linear form $p_i^\star$ may be extended by Banach Theorem to the space $\mathrm{C}^{l_i}([\xi_{1,0}, \xi_{1,1}])$, with $0 \leq l_i < k$, such that we may still assume:

$$|p_i^\star(v)| \lesssim \|v\|_{\mathrm{C}^{l_i}([\xi_{1,0},\xi_{1,1}])} \quad \forall v \in \mathrm{C}^{l_i}([\xi_{1,0}, \xi_{1,1}]). \tag{3.24}$$

It is seen that the former hypothesis, *i.e.*, equation (3.24), is generally satisfied in practice since the linear maps ϕ_{ij} and ψ_{ij} are generally of the form $\frac{\partial^{p+q}}{\partial \xi_1^p \xi_2^q}$ (see for instance Example 3.2). From now on, we shall systematically assume that (3.24) holds on the space $\mathrm{C}^k([\xi_{1,0}, \xi_{1,1}])$ and it is seen that the maps ϕ_{ij} and ψ_{ij} may be naturally extended *via* equation (3.23) to every function w (sufficently smooth function) defined on $\mathbf{K}$ and $2\pi R$-periodic with respect to the variable ξ_2 such that $w(., \xi_2)$ and $\frac{\partial w}{\partial \xi_2}(., \xi_2)$ belong to the space $\mathrm{C}^k([\xi_{1,0}, \xi_{1,1}])$ for every ξ_2. More specifically, we have:

$$\begin{cases} \phi_{ij}(w) = p_i^\star(w(., \xi_{2,j})) \\ \psi_{ij}(w) = p_i^\star(\frac{\partial w}{\partial \xi_2}(., \xi_{2,j})). \end{cases} \tag{3.25}$$

Similarly, we shall assume that equations (3.24) and (3.25) hold for the same function w when the reference element is considered with the following identity:

$$\begin{cases} \phi_{ij}(w) = \hat{\phi}_{ij}(\hat{w}) & \forall i, j \\ \psi_{ij}(w) = \hat{\psi}_{ij}(\hat{w}) & \forall i, j \end{cases} \tag{3.26}$$

where $\hat{w} = w \circ \mathbf{F_K}$.

Example 3.4. If $\mathbb{P}_1$ is considered, ϕ_{ij} and ψ_{ij} are extended as follow for suitable smooth function w:

$$\begin{cases} \phi_{ij}(w) = w\left(\xi_{1,i}, \xi_{2,j}\right) & \forall\ i = 0, 1 \quad 0 \leq j \leq N_2 \\ \psi_{ij}(w) = \frac{\partial w}{\partial \xi_2}\left(\xi_{1,i}, \xi_{2,j}\right) & \forall\ i = 0, 1 \quad 0 \leq j \leq N_2. \end{cases} \tag{3.27}$$

If $\mathbb{P}_3$ is considered, we take:

$$\begin{cases} \phi_{ij}(w) = w\left(\xi_{1,i}, \xi_{2,j}\right) & \forall\ 0 \leq i \leq 1 \quad 0 \leq j \leq N_2 \\ \phi_{ij}(w) = \frac{\partial w}{\partial \xi_1}\left(\xi_{1,i-2}, \xi_{2,j}\right) & \forall\ 2 \leq i \leq 3 \quad 0 \leq j \leq N_2 \\ \psi_{ij}(w) = \frac{\partial w}{\partial \xi_2}\left(\xi_{1,i}, \xi_{2,j}\right) & \forall\ 0 \leq i \leq 1 \quad 0 \leq j \leq N_2 \\ \psi_{ij}(w) = \frac{\partial^2 w}{\partial \xi_1 \partial \xi_2}\left(\xi_{1,i-2}, \xi_{2,j}\right) & \forall\ 2 \leq i \leq 3 \quad 0 \leq j \leq N_2. \end{cases} \tag{3.28}$$

□

Since the linear forms ϕ_{ij} and ψ_{ij} are defined for sufficiently regular maps, we end this part by introducing the local interpolant operators $\Pi_{\mathbf{K}}$ and $\hat{\Pi}_{\hat{\mathbf{K}}}$, associated with smooth functions, used to define the global interpolant in the next section.

Definition 3.5. The local interpolant operator $\hat{\Pi}_{\hat{\mathbf{K}}}$ on the reference element $\hat{\mathbf{K}}$ is defined by:

$$\hat{\Pi}_{\hat{\mathbf{K}}}\hat{w} = \sum_{ij} \hat{\phi}_{ij}(\hat{w})\hat{p}_i \otimes \hat{t}_j + \sum_{ij} \hat{\psi}_{ij}(\hat{w})\hat{p}_i \otimes \hat{s}_j \tag{3.29}$$

for every $\hat{w}$ a k-times continuously differentiable on $\hat{\mathbf{K}}$ and 2π-periodic with respect to the second variable. Similarly, if $w = \hat{w} \circ \mathbf{F}_{\mathbf{K}}^{-1}$, we adopt the following generalization:

$$\Pi_{\mathbf{K}} w = \sum_{ij} \phi_{ij}(w) p_i \otimes t_j + \sum_{ij} \psi_{ij}(w) p_i \otimes s_j. \tag{3.30}$$

In particular, using (3.26), one may observe that:

$$\Pi_{\mathbf{K}} w = \hat{\Pi}_{\hat{\mathbf{K}}}\hat{w} \circ \mathbf{F}_{\mathbf{K}}^{-1}. \tag{3.31}$$

Remark 3.6. It is important to note that the definition of the interpolant in Definition 3.5 does not necessarily imply that $\Pi_{\mathbf{K}} w \in \mathbf{P}_{\mathbf{K}}^{[k,N_2]}$.

4. Discretized problem and Convergence analysis

In this section, we aim to achieve two goals. First, we will introduce the discretized version of problem $(\mathcal{P})$ and describe the numerical method used to solve it. Second, we will study error estimates for the solution under certain assumptions about its regularity. We will assume throughout this section that the hypothesis (**Hr**) holds.

4.1. Discretized problem

To begin, we consider a family of discretizations of the domain $\bar{\Omega}$ denoted by $(\mathcal{S}(h))_h$ such that the mid-surface in the reference configuration is discretized as $\bar{\Sigma} = \cup_{i,j}[\xi_{1,i-1}, \xi_{1,i}] \times [\xi_{2,j-1}, \xi_{2,j}] = \cup_i \mathbf{K}_i$ with $\mathbf{K}_i = [\xi_{1,i-1}, \xi_{1,i}] \times [0, 2\pi R]$ (see Fig. 3), where:

- $\Psi([0, L])$ is partitioned into elements $\cup_{i=1}^{N_1} e_i$ where $e_i = \Psi\left([\xi_{1,i-1}, \xi_{1,i}]\right)$ and $0 = \xi_{1,0} < \xi_{1,1} < \cdots < \xi_{1,N_1} = L$. The mesh size bounds are $h_{\max}$ and $h_{\min}$ are defined by $h_{\max} = \max\limits_{1 \leq i \leq N_1}(\xi_{l,i} - \xi_{l,i-1}) > 0$ and $h_{\min} = \min\limits_{1 \leq i \leq N_1}(\xi_{l,i} - \xi_{l,i-1}) > 0$.
- Each section of the mid-surface is parametrized by $\mathcal{C}_i : \xi_2 \to \Theta(\xi_1 = \xi_{1,i}, \xi_2, \xi_3 = 0)$ and splitted into N_2 elements as $\mathcal{C}_i = \cup_{j=1}^{N_2} c_j$, where $c_j = \mathcal{C}_i\left([\xi_{2,i-1}, \xi_{2,i}]\right)$ and $0 = \xi_{2,0} < \xi_{2,1} < \cdots < \xi_{2,N_2} < 2\pi R$ the same discrete coordinates defined in (3.10).

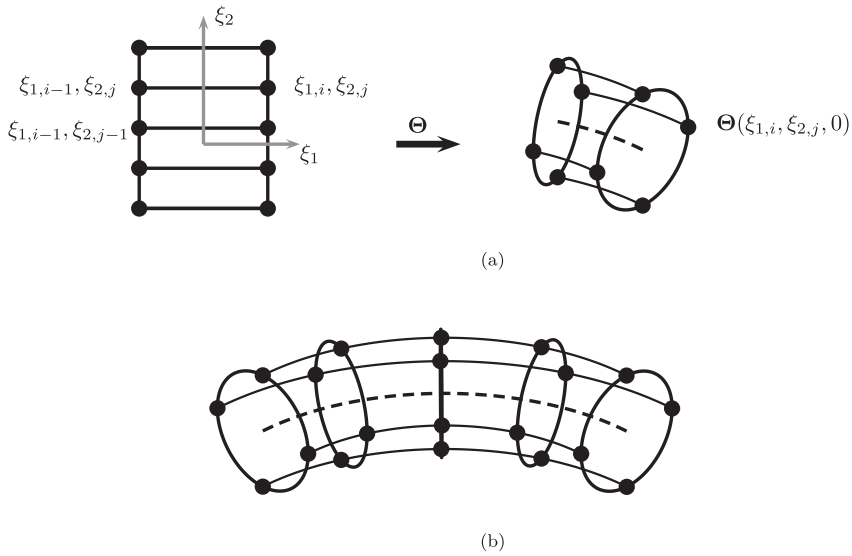

FIGURE 3. (a) Finite element in the curvilinear frame (left) and the corresponding finite element in the Cartesian frame (right) (b) Pipe mid-surface divided into several elements, *i.e.*, $\cup_i \Theta(\mathbf{K}_i \times \{0\})$, in the Euclidean space.

Given a discretization $\mathcal{S}(h)$ as described above, we shall deal with the spatial discretized problem $(\mathcal{P}_h)$ associated with $(\mathcal{P})$ and consists on finding $\mathbf{u}_h = (u_{l,h})_{1\leq l\leq 3} \in \mathbf{V_h}(\Sigma)$ such that:

$$\mathbf{a}(\mathbf{u}_h, \mathbf{v}_h) = \int_\Omega \mathbf{A}^{ijkl} e_{i\|j}(\mathbf{u}_h) e_{k\|l}(\mathbf{v}_h)\sqrt{g}dx = \int_{\Gamma_1} \mathbf{h}\cdot\gamma\mathbf{T}\mathbf{v}_h\sqrt{g}\,d\Gamma \quad \forall \mathbf{v}_h \in \mathbf{V_h}(\Sigma) \tag{4.1}$$

where the finite dimensional space $\mathbf{V_h}(\Sigma) \subset \mathbf{V}(\Sigma)$ is defined by:

$$\mathbf{V_h}(\Sigma) = \left\{ \mathbf{v}_h \in \mathbf{V}(\Sigma) \mid \mathbf{v}_h{}_{|\mathbf{K}_j} \circ \mathbf{F}_{\mathbf{K}_j} \in \mathbf{P}_{\hat{\mathbf{K}}}^{[k_1,N_2]} \times \mathbf{P}_{\hat{\mathbf{K}}}^{[k_2,N_2]} \times \mathbf{P}_{\hat{\mathbf{K}}}^{[k_3,N_2]} \right\} \tag{4.2}$$

with $k_1, k_2 \geq 1$ and $k_3 \geq 3$. Depending on the choice of the boundary conditions on Γ_0, it may happen that the space $\mathbf{V_h}(\Sigma)$ is reduced to the single element $\{0\}$, for instance, by selecting $\Gamma_0 = (0, L) \times J \times \frac{e}{2}$, with J being an open interval in $(0, 2\pi R)$. Indeed, if $\mathbf{v}_h = (v_{i,h})_{1\leq i\leq 3} \in \mathbf{V_h}(\Sigma)$, the expression (2.8) combined with t he fact that we are dealing with polynomials lead to $v_{3,h} = 0$, resulting in $v_{1,h} = v_{2,h} = 0$ using the expressions (2.12). Henceforth, we will assume that the space $\mathbf{V_h}(\Sigma)$ is different from $\{0\}$ and is endowed with the induced norm as a subspace of $\mathbf{V}(\Sigma)$. In the formulation (4.1), the numerical computation of the local integrals:

$$\int_{\Omega_e} \mathbf{A}^{ijkl} e_{i\|j}(\mathbf{u}_h) e_{k\|l}(\mathbf{v}_h)\sqrt{g}dx \tag{4.3}$$

is performed *via* the Gauss integration with respect to ξ_1, ξ_3 and the Tchebychev integration with respect ξ_2, where the parameter N in Lemma 3.3 is taken greater or equal to $2N_2 + 1$. The strategy to solve $\mathcal{P}_h$, is to approximate each component of $\mathbf{u}_h{}_{|\mathbf{K}_e}$ by an element in the span $\{p_i^{(l)} \otimes t_j, p_i^{(l)} \otimes s_j\}_{(i,j)\in \mathbf{I}_{\hat{\mathbf{K}}}}$, where $(p_i^{(l)})_i$ being a basis of the space $\mathbb{P}_{k_l}$, and then the constraints in Lemma 3.3 (2) are enforced *via* the mixed method using the Lagrange multipliers such that the problem $\mathcal{P}_h$ can be cast in the following linear system:

$$\begin{bmatrix} \mathbb{K} & \mathbb{L}^T \\ \mathbb{L} & 0 \end{bmatrix} \begin{bmatrix} \mathbb{U} \\ \lambda \end{bmatrix} = \begin{bmatrix} \mathbb{F} \\ 0 \end{bmatrix} \tag{4.4}$$

where $\mathbb{K}$ is a symmetric positive matrix, $\mathbb{L}$ is the constraint matrix to ensure the constraints in Lemma 3.3 (2) as well as the Dirichlet conditions (assumed zero in (4.4)), $\mathbb{U}$ represents the vector of degrees of freedom and λ the Lagrange multipliers. Recall that the conditions on each element $\mathbf{K}_m$, described in Lemma 3.3 (2), are imposed through the operator $\mathbb{L}$ as follows:

$$\sum_{j=0}^{N_2} \psi_{ij}^{l,m}\left(u_{l,h}|_{\mathbf{K}_m}\right) = 0 \quad \forall\, 0 \le i \le k_l, 1 \le l \le 3. \tag{4.5}$$

Here, the linear forms $\psi_{ij}^{l,m}$ are associated to the finite element $\left(\mathbf{K}_m, \mathbf{P}_{\mathbf{K}_m}^{[k_l,N_2]}, \mathbf{T}_{\mathbf{K}_m}^{\star}\right)$. It is important to emphasize that the matrix $\mathbb{L}$ should be onto as a necessary condition for the well-posedness of the saddle point problems. In other words, the constraints in Lemma 3.3 (2) should be independent of the constraints imposed physically as the Dirichlet conditions. The former independence may fail, for instance, if one choose to impose (as Dirichlet conditions) $\psi_{ij}^{l,m}\left(u_{l,h}|_{\mathbf{K}_m}\right) = 0$ for every j and for a fixed i, l and m. The surjectivity of $\mathbb{L}$ can be verified, for instance, by computing the singular values. Moreover, if the operator $\mathbb{L}$ is onto, the problem (4.4) is well-posed since $\mathbf{u}_h \in \mathbf{V_h}(\Sigma) \subset \mathbf{V}(\Sigma)$, and invoking Lemma 3.3 (1) along with the coercivity of the bilinear form discussed in Lemma 2.1.

Given the dependency of $\mathbb{L}$ on discretization parameters, it is important to examine the stability of the system (4.4) within the context of inf-sup conditions. This examination deals with the uniform boundedness of the coercivity constant of $\mathbb{L}$ with respect to the discretization parameters. The following lemma addresses this concern, focusing on a particular case of Dirichlet conditions frequently encountered in practical scenarios, as illustrated in the subsequent numerical examples.

Lemma 4.1. *Assume that* $\mathbb{L} = \begin{bmatrix} \mathbb{L}_1 \\ \mathbb{L}_2 \end{bmatrix}$ *such that:*

- $\mathbb{L}_1$ *is associated with the conditions* (4.5)
- *Each row of the matrix* $\mathbb{L}_2 \neq 0$ *is zero everywhere except for exactly one entry, which is set to 1.*

If $\mathbb{L}$ *is surjective, then the smallest singular value of* $\mathbb{L}^T$ *is given by:*

$$\frac{N_2 + 2 - \sqrt{N_2^2 + 4\alpha}}{2} \tag{4.6}$$

for some positive integer $0 \le \alpha \le N_2$

Proof. Using a permutation process, $\mathbb{L}$ is equivalent to the following matrix:

$$\begin{bmatrix} \mathbb{I} & & & & \\ & \mathbb{J}_0 & & & \\ & & \mathbb{J}_1 & & \\ & & & \ddots & \\ & & & & \mathbb{J}_N \end{bmatrix} \tag{4.7}$$

where $N = (N_1+1)\sum_{l=1}^{3}(k_l+1)$, $\mathbb{I}$ is an identity matrix and for every $0 \le j \le N$, $\mathbb{J}_j$ is $(\alpha_j+1)\times(N_2+1)$ matrix characterized by:

- The first row is unity everywhere
- The other rows (if $\alpha_j \ge 1$) are zero everywhere expect for exactly one entry, which is 1

It is seen that the surjectivity of $\mathbb{L}$ implies that $\alpha_j \leq N_2$. By induction on N_2, it can be established that the singular values of $\mathbb{J}_j^T$ are exactly:

$$\begin{cases} N_2+1 & \text{if } \alpha_j = 0 \\ \frac{N_2+2-\sqrt{N_2^2+4}}{2}, \quad \frac{N_2+2+\sqrt{N_2^2+4}}{2} & \text{if } \alpha_j = 1 \\ 1, \quad \frac{N_2+2-\sqrt{N_2^2+4\alpha_j}}{2}, \quad \frac{N_2+2+\sqrt{N_2^2+4\alpha_j}}{2} & \text{if } \alpha_j \geq 2. \end{cases} \tag{4.8}$$

Observing that $\frac{N_2+2-\sqrt{N_2^2+4\alpha}}{2} = 1$ holds when $\alpha = 0$, and taking into account that $0 < \frac{N_2+2-\sqrt{N_2^2+4\alpha_j}}{2} \leq 1$ and $\mathbb{L}_2 \neq 0$, this completes the proof. □

From the proof of Lemma 4.1, two interesting observations can be derived:

- If the ratios $\left(\frac{\alpha_j}{N_2}\right)_{0\leq j\leq N}$ are uniformly bounded by a constant in the interval $[0,1)$, then it holds that $\|\mathbb{L}^T\lambda\| \geq \delta\|\lambda\|$ with $\delta > 0$, independent of the discretization parameters.
- In the specific case, where $\alpha \sim N_2$ as $N_2 \to \infty$, we find that $\frac{N_2+2-\sqrt{N_2^2+4\alpha}}{2} \to 0$. In this case, the system (4.4) tends to degenerate, potentially resulting in accuracy issues for large values of N_2. However, given that the main purpose of the pipe elements is to achieve acceptable accuracy using small values of N_2 (typically less than 10), the use of the formulation may still yield satisfactory results (see the numerical examples below).

4.2. Error estimates and convergence analysis

In this section, we will derive error estimates for the discrete version of the problem $(\mathcal{P})$. Our analysis will be based on the the following functional spaces: Let $a > 0$, r a positive integer and $\mathbf{X}$ an arbitrary Banach space, we define:

- $\mathrm{L}^p(0,a;\mathbf{X})$, with $1 \leq p$, is the set of $\mathbf{X}$-valued Bochner integrable functions $u : (0,a) \to \mathbf{X}$ such that $\int_J \|u\|_{\mathbf{X}}^p < \infty$.
- $\mathrm{L}^\infty(0,a;\mathbf{X})$ is the space of (strong) measurable functions u bounded almost everywhere on $(0,a)$ and equipped with the norm $\|u\|_{\mathrm{L}^\infty(0,a;\mathbf{X})} = \inf\{C \geq 0 : \|u(x)\|_{\mathbf{X}} \leq C \quad a.e.\}$.
- $\mathrm{H}^m(0,a;\mathbf{X})$, the set of functions $u : (0,a) \to \mathbf{X}$ such that $u \in \mathrm{L}^2(0,a;\mathbf{X})$ and $u^{(k)} \in \mathrm{L}^2(0,a;\mathbf{X})$, here the derivative $u^{(k)}$ is understood in the sense of distributions [10].
- $\mathrm{C}^r_{per}(0,a;\mathbf{X})$ is the space of r-times continuously differentiable (vector-valued) functions on $\mathbb{R}$ and a-periodic equipped with the norm $\|v\|_{\mathrm{C}^r_{per}(0,a;\mathbf{X})} = \sum_{0\leq k\leq r} \max_{s\in[0,a)} \|v^{(k)}(s)\|_{\mathbf{X}}$.

Furthermore, using the definition of the local interpolant in Definition 3.5, we introduce the global interpolant associated with a discretization $\mathcal{S}(h)$:

Definition 4.2. Given a discretization $\bar{\Sigma} = \cup_i \mathbf{K}_i$ with the associated finite elements $\left(\mathbf{K}_i, \mathbf{P}_{\mathbf{K}_i}^{[k,N_2]}, \mathbf{T}_{\mathbf{K}_i}^\star\right)$, we consider w as a k-times continuously differentiable on $\bar{\Sigma}$ and 2π-periodic with respect to the second variable. The global interpolant related to w is the function $\Pi_h w$ defined on $\bar{\Sigma}$ such that:

$$(\Pi_h w)_{|\mathbf{K}_i} = \Pi_{\mathbf{K}_i} w_{|\mathbf{K}_i} \quad \forall\, i. \tag{4.9}$$

□

Remark 4.3. Given the finite elements $\left(\mathbf{K}_i, \mathbf{P}_{\mathbf{K}_i}^{[k,N_2]}, \mathbf{T}_{\mathbf{K}_i}^\star\right)_i$ as in Definition 4.2 and k-times continuously differentiable function w on $\bar{\Sigma}$ with $k \geq 1$, the expression of the global interpolant $\Pi_h w$ does not ensure the continuity on $\bar{\Sigma}$. More specifically, it may happen that $\Pi_{\mathbf{K}_i} w_{|\partial\mathbf{K}_i\cap\partial\mathbf{K}_j} \neq \Pi_{\mathbf{K}_j} w_{|\partial\mathbf{K}_i\cap\partial\mathbf{K}_j}$ or even for the derivatives, for some i,j such that $\partial\mathbf{K}_i \cap \partial\mathbf{K}_j \neq \emptyset$. For this purpose, we shall always assume the following on the operator Π_h:

$(\mathbf{H}_\Pi)$: For every $w \in \mathrm{C}^k(\bar{\Sigma})$ (with $k \geq 1$)

– $\Pi_h w \in \mathrm{H}^1(\bar{\Sigma})$ if $k = k_1, k_2$ and $\mathrm{H}^2(\bar{\Sigma})$ if $k = k_3$

The assumption $(\mathbf{H}_\Pi)$ is usually adopted in practice, in particular for the linear forms $(\phi_{ij})_{ij}$ and $(\psi_{ij})_{ij}$ defined above in Example 3.4.

□

The main result of this section is the following:

Theorem 4.4. *Consider the domain Ω as described in Section 2. With the notation of Section 4.1, we still consider $\mathbf{u} = (u_i)_{1\le i\le 3}$ and $\mathbf{u}_h = (u_{i,h})_{1\le i\le 3}$ as the solutions of the problems $(\mathcal{P})$ and $(\mathcal{P}_h)$, respectively. Moreover, we assume the existence of a positive integer $p_i > k_i$, with $1 \le i \le 3$, such that:*

(1) $0 < h_{min} \le h_{\max} < R$
(2) $N_2 \ge 2$
(3) $u_i \in \mathrm{L}^2(0, 2\pi R; \mathrm{H}^{p_i}(0, L))$, *i.e.,* $u_i(., \xi_2) \in \mathrm{H}^{p_i}(0, L)$ *a.e.*
(4) If $\mathbf{c}_{i,n} = \frac{1}{2\pi R}\int_0^{2\pi R} u_i(., \xi_2) e^{-i_c \frac{n\xi_2}{R}}\, d\xi_2$, *we have:*

$$0 \le \limsup_n \sqrt[n]{\|\mathbf{c}_{i,n}\|_{\mathrm{H}^{p_i}(0,1)}} < 1 \tag{4.10}$$

(5) $\mathbf{T}\Pi_h\mathbf{u} = 0$ *on* Γ_0, *where* $\Pi_h\mathbf{u} = (\Pi_h u_i)_{1\le i\le 3}$

where i_c stands for the imaginary unit. Then, under the assumption $(\mathbf{H}_\Pi)$ and for sufficiently small $h_{\max}$, there exits a constant $b > 0$ such that for every integer $r > \max\limits_{1\le i\le 3} k_i$:

$$\|\mathbf{u}_h - \mathbf{u}\|_{\mathbf{V}(\Sigma)} \le \mathfrak{C}\frac{N_2^2}{h_{\min}^2}\left[\frac{1}{\sinh^2\left(\frac{N_2+1}{2}b\right)} + h_{\min}^2 \max_{1\le i\le 3} h_{\max}^{p_i-2} + \max_{1\le i\le 3}\frac{1}{N_2^{r-k_i-1}}\right] \tag{4.11}$$

where the constant $\mathfrak{C}$ is independent of the discretization parameters, i.e., N_2, $h_{\min}$ and $h_{\max}$, but depends on the parameter r and the geometric characteristics of the pipe.

According to Theorem 4.4, it is seen that the discrete solution converges to the exact solution if the parameters r and p_i $(1 \le i \le 3)$ are sufficiently large and the discretization parameters are appropriately chosen. In particular, the following result is only a direct consequence of Theorem 4.4:

Corollary 4.5. *For every $\alpha, \beta > 0$ with $\alpha \ge 1$, we define the set $\mathbf{S}(\alpha, \beta)$:*

$$\mathbf{S}(\alpha,\beta) = \{(h_{\max}, h_{\min}, N_2) \in \mathbb{R}^+ \times \mathbb{R}^+ \times \mathbb{N} \mid \beta \le \frac{h_{\min}}{h_{\max}} \le \alpha \quad \text{and} \quad \beta \le N_2 h_{\max} \le \alpha\}. \tag{4.12}$$

Let $(\mathbf{x}_l)_l \in \mathbf{S}(\alpha,\beta)^{\mathbb{N}}$ a sequence converging to $(0, 0, \infty)$ and denotes $(\mathbf{u}_{h_l})_l$ the sequence of the corresponding discrete solutions. Under the assumptions of Theorem 4.4, we have:

$$\lim_l \|\mathbf{u}_{h_l} - \mathbf{u}\|_{\mathbf{V}(\Sigma)} = 0 \tag{4.13}$$

for $r > \max\limits_{1\le i\le 3} k_i + 5$ and $\min\limits_{1\le i\le 3} p_i > 4$.

Now, we will prove Theorem 4.4 by establishing three lemmas. For simplicity, we will frequently use the notation $\mathfrak{C}$ in the proofs below to refer to an arbitrary constant that is independent of the discretization parameters N_2, $h_{\min}$, and $h_{\max}$.

Lemma 4.6. *Let $\hat{f} : \mathbb{R} \to \mathbf{X}$ a 2π-periodic such that $\hat{f} \in \mathrm{L}^2(0, 2\pi; \mathbf{X})$, where $\mathbf{X}$ is a Hilbert space. Assume that:*

$$0 \leq \limsup_n \sqrt[n]{\|\hat{\mathbf{c}}_n\|_{\mathbf{X}}} < 1 \tag{4.14}$$

where:

$$\hat{\mathbf{c}}_n = \frac{1}{2\pi} \int_0^{2\pi} \hat{f}(s) e^{-i_c n s} \, ds. \tag{4.15}$$

Let $T_{N_2}(\hat{f})$ defined by:

$$T_{N_2}(\hat{f}) = \sum_{j=0}^{N_2} \hat{f}\left(\hat{\xi}_{2,j}\right) \hat{t}_j + \sum_{j=0}^{N_2} \hat{f}'\left(\hat{\xi}_{2,j}\right) \hat{s}_j. \tag{4.16}$$

Then, there exists a constant $b > 0$, depending only on $\hat{f}$, such that for every $q \in \{0, 1, 2, \ldots\}$:

$$\|\hat{f}^{(q)} - T_{N_2}(\hat{f})^{(q)}\|_{\mathrm{L}^\infty(0,2\pi;\mathbf{X})} \leq C(\hat{f}, b, \mathbf{X}) q! \, (2(N_2+1))^q \, \frac{\coth^{q+1}(\frac{b}{2})}{\sinh^2\left(\frac{N_2+1}{2} b\right)} \tag{4.17}$$

where $C(\hat{f}, b, \mathbf{X}) = \left(\sum_{n=-\infty}^{\infty} \|\hat{\mathbf{c}}_n\|_{\mathbf{X}}^2 e^{2nb} \right)^{\frac{1}{2}}$

Proof. The proof mainly follows the ideas of [13] with some modifications. According to the hypothesis of Lemma 4.6, we have $\hat{f} \in \mathrm{L}^2(0, 2\pi; \mathbf{X})$, which implies, using for instance Theorem 1.6 in [1], that:

$$\hat{f}(u) = \sum_{n=-\infty}^{\infty} \hat{\mathbf{c}}_n e^{i_c n u} \quad \forall u \in [0, 2\pi]. \tag{4.18}$$

Let $x^\star \in X^\star$, it is seen that we can write $x^\star \circ \hat{f}$ as:

$$x^\star \circ \hat{f}(u) = \sum_{n=-\infty}^{\infty} x^\star(\hat{\mathbf{c}}_n) e^{i_c n u} \quad \forall u \in [0, 2\pi] \tag{4.19}$$

since $\sum_{n=-\infty}^{\infty} \hat{\mathbf{c}}_n e^{i_c n u}$ is unconditionally convergent. By virtue of (4.14), the function $g(z) = \sum_{n=-\infty}^{\infty} x^\star(\hat{\mathbf{c}}_n) e^{i_c n z}$ is 2π-periodic analytic function on the strip $\mathbf{B} = \{z \in \mathbb{C} \mid -b < \Im(z) < b\}$ and continuous on $\bar{\mathbf{B}}$, for some $b > 0$ independent of $x^\star$, *i.e.*, b may be chosen, for instance, such that $\sum_{n=-\infty}^{\infty} \|\hat{\mathbf{c}}_n\|_{\mathbf{X}} e^{nb} < \infty$ since (4.14) holds.

The next step is to estimate an upper bound of $g(z) - T_{N_2}(g)(z)$, where we extend the definition of $T_{N_2}(g)$ as follows:

$$T_{N_2}(g)(z) = \sum_{j=0}^{N_2} g\left(\hat{\xi}_{2,j}\right) \hat{t}_j(z) + \sum_{j=0}^{N_2} g'\left(\hat{\xi}_{2,j}\right) \hat{s}_j(z). \tag{4.20}$$

Here $(\hat{s}_j)_j$ and $(\hat{t}_j)_j$ are defined on the complex plane with the trivial analytical extension. Notice that $T_{N_2}(\hat{f}) = T_{N_2}(g)_{|\Im(z)=0}$. Following the same argument in [13], we obtain:

$$g(z) - T_{N_2}(g)(z) = \frac{\sin^2(\frac{N_2+1}{2} z)}{4\pi i_c} \left(\int_{-i_c b}^{2\pi - i_c b} \frac{\cot\left(\frac{\xi - z}{2}\right)}{\sin^2\left(\frac{N_2+1}{2}\xi\right)} g(\xi) \, d\xi - \int_{i_c b}^{2\pi + i_c b} \frac{\cot\left(\frac{\xi - z}{2}\right)}{\sin^2\left(\frac{N_2+1}{2}\xi\right)} g(\xi) \, d\xi \right) \quad \forall z \in \mathbf{B}. \tag{4.21}$$

Moreover, refering again to the arguments of [13], we have for every $q \in \{0,1,2,\ldots\}$:

$$\begin{cases} |\frac{d^q}{dz^q}\sin^2(\frac{N_2+1}{2}z)\cot\frac{\xi-z}{2}| \leq q!(2(N_2+1))^q\coth^{q+1}(\frac{b}{2}) \quad \forall z\in\mathbb{R} \\ \sinh\frac{N_2+1}{2}b \leq |\sin\frac{N_2+1}{2}\xi|. \end{cases} \tag{4.22}$$

Thus, combining the equality $\|\hat{f}^{(q)}(z) - T_{N_2}(\hat{f})^{(q)}(z)\|_{\mathbf{X}} = \sup_{x^\star\in\mathcal{B}_{\mathbf{X}^\star}} |x^\star\circ\hat{f}^{(q)}(z) - x^\star\circ T_{N_2}(\hat{f})^{(q)}(z)|$, for every $z\in\mathbb{R}$, with the Cauchy inequality, yields the desired result and this completes the proof.

□

Lemma 4.7. *With the same notations of Section 3, consider the finite element* $\left(\hat{\mathbf{K}}, \mathbf{P}_{\hat{\mathbf{K}}}^{[k,N_2]}, \mathbf{T}_{\hat{\mathbf{K}}}^\star\right)$ *and a function* $\hat{v}\in \mathrm{C}^r_{per}(0,2\pi;\mathrm{C}^k[0,1])$ *with* $k\leq r$*, i.e.,* $\frac{\partial^j\hat{v}}{\partial\hat{\xi}_2^j}(.,\hat{\xi}_2)\in\mathrm{C}^k[0,1]$ *for every* $0\leq j\leq r$*. If* $N_2\geq 2$*, we have:*

$$\left|\frac{1}{N_2+1}\sum_{j=0}^{N_2}\hat{\psi}_{ij}(\hat{v})\right| \leq \frac{\mathfrak{C}}{N_2^{r-l_i-1}}\|\hat{v}\|_{\mathrm{C}^r_{per}(0,2\pi;\mathrm{C}^k[0,1])} \tag{4.23}$$

for every $0\leq i\leq k$*. The constant* $\mathfrak{C}$ *may depend on* r*.*

Proof. Let $0\leq i\leq k$. According to the discussion in Section 3, we have:

$$\begin{aligned} \frac{1}{N_2+1}\left|\sum_{j=0}^{N_2}\hat{\psi}_{ij}(\hat{v})\right| &= \frac{1}{N_2+1}\left|\sum_{j=0}^{N_2}\hat{p}_i^\star\left(\frac{\partial\hat{v}}{\partial\hat{\xi}_2}\left(.,\hat{\xi}_{2,j}\right)\right)\right| \\ &\lesssim \left\|\frac{1}{N_2+1}\sum_{j=0}^{N_2}\frac{\partial\hat{v}}{\partial\hat{\xi}_2}\left(.,\hat{\xi}_{2,j}\right)\right\|_{\mathrm{C}^{l_i}([\xi_{1,0},\xi_{1,1}])}. \end{aligned} \tag{4.24}$$

Select $\hat{\xi}_1\in[0,1]$ and a positive integer $0\leq j\leq l_i<k$. By virtue of Theorem 13.6 chapter III in [21], we choose $A_{r,j}$ as a constant depending only on r and j such that:

$$\inf_{T\in\mathbb{T}_{N_2}}\max_{\hat{\xi}_2\in[0,2\pi]}\left|\frac{\partial^{j+1}\hat{v}}{\partial\hat{\xi}_1^j\partial\hat{\xi}_2}\left(\hat{\xi}_1,\hat{\xi}_2\right) - T(\hat{\xi}_2)\right| \leq \frac{A_{r,j}\left\|\frac{\partial^r\hat{v}}{\partial\hat{\xi}_1^j\partial\hat{\xi}_2^{r-j}}\right\|_{\infty,\hat{K}}}{N_2^{r-j-1}}. \tag{4.25}$$

Let $\epsilon>0$ and $T\in\mathbb{T}_{N_2}$ such that:

$$\max_{\hat{\xi}_2\in[0,2\pi]}\left|\frac{\partial^{j+1}\hat{v}}{\partial\hat{\xi}_1^j\partial\hat{\xi}_2}\left(\hat{\xi}_1,\hat{\xi}_2\right) - T(\hat{\xi}_2)\right| \leq \frac{(A_{r,j}+\epsilon)\left\|\frac{\partial^r\hat{v}}{\partial\hat{\xi}_1^j\partial\hat{\xi}_2^{r-j}}\right\|_{\infty,\hat{K}}}{N_2^{r-j-1}}. \tag{4.26}$$

Then:

$$\begin{aligned} \frac{1}{N_2+1}\sum_{l=0}^{N_2}\frac{\partial^{j+1}\hat{v}}{\partial\hat{\xi}_1^j\partial\hat{\xi}_2}\left(\hat{\xi}_1,\hat{\xi}_{2,l}\right) = \frac{1}{N_2+1}\sum_{l=0}^{N_2}\left(\frac{\partial^{j+1}\hat{v}}{\partial\hat{\xi}_1^j\partial\hat{\xi}_2}\left(\hat{\xi}_1,\hat{\xi}_{2,l}\right) - T(\hat{\xi}_{2,l})\right) + \\ \frac{1}{2\pi}\int_0^{2\pi}\left(\frac{\partial^{j+1}\hat{v}}{\partial\hat{\xi}_1^j\partial\hat{\xi}_2}(\hat{\xi}_1,\hat{\xi}_2) - T(\hat{\xi}_2)\right)d\hat{\xi}_2. \end{aligned} \tag{4.27}$$

Indeed, according to Lemma 3.19, we have:

$$\frac{1}{N_2+1}\sum_{l=0}^{N_2}T(\hat{\xi}_{2,l}) = \frac{1}{2\pi}\int_0^{2\pi}T(\hat{\xi}_2)d\hat{\xi}_2 \tag{4.28}$$

and, by the periodicity of $\frac{\partial^j \hat{v}}{\partial \hat{\xi}_1^j}$:

$$\int_0^{2\pi} \frac{\partial^{j+1}\hat{v}}{\partial \hat{\xi}_1^j \partial \hat{\xi}_2}\, d\hat{\xi}_2 = 0. \tag{4.29}$$

Using (4.26) and the fact that ϵ is arbitrary, we deduce that:

$$\max_{\hat{\xi}_1} \left| \frac{1}{N_2+1} \sum_{l=0}^{N_2} \frac{\partial^{j+1}\hat{v}}{\partial \hat{\xi}_1^j \partial \hat{\xi}_2} \left(\hat{\xi}_1, \hat{\xi}_{2,l}\right) \right| \leq \frac{2A_{r,j} \| \frac{\partial^r \hat{v}}{\partial \hat{\xi}_1^j \partial \hat{\xi}_2^{r-j}} \|_{\infty,\hat{K}}}{N_2^{r-j-1}}. \tag{4.30}$$

Using the inequality $\sum_{j=0}^{l_i} \frac{1}{N_2^{r-j-1}} \leq \frac{2}{N_2^{r-l_i-1}}$ for $N_2 \geq 2$, we get the desired result. □

Lemma 4.8. *Consider the reference finite element* $\left(\hat{\mathbf{K}}, \mathbf{P}_{\hat{\mathbf{K}}}^{[k,N_2]}, \mathbf{T}_{\hat{\mathbf{K}}}^{\star}\right)$ *with* $N_2 \geq 2$. *Let* p *a positive integer with* $k < p$ *and* $\hat{v}$ *a function defined on* $\hat{\mathbf{K}}$ *such that:*
(1) $\hat{v} \in \mathrm{L}^2(0, 2\pi; \mathrm{H}^p(0,1))$, *i.e.,* $\hat{v}(., \hat{\xi}_2) \in \mathrm{H}^p(0,1)$ *a.e.*
(2) If $\hat{\mathbf{c}}_n = \frac{1}{2\pi} \int_0^{2\pi} \hat{v}(., \hat{\xi}_2) e^{-i_c n \hat{\xi}_2}\, d\hat{\xi}_2$, *we have:*

$$0 \leq \limsup_n \sqrt[n]{\|\hat{\mathbf{c}}_n\|_{\mathrm{H}^p(0,1)}} < 1 \tag{4.31}$$

then, there exists $b > 0$ *such that for* $0 \leq l \leq k$:

$$\begin{aligned} |\hat{v} - \hat{\Pi}_{\hat{\mathbf{K}}} \hat{v}|_{2,l,\hat{\mathbf{K}}} \leq \mathfrak{C} \Bigg[& \left(\sum_{n=-\infty}^{\infty} \|\hat{\mathbf{c}}_n\|^2_{\mathrm{H}^p(0,1)} e^{nb} \right)^{\frac{1}{2}} \frac{(N_2+1)^l}{\sinh^2(\frac{N_2+1}{2} b)} + \\ & \frac{N_2^{l+1}-1}{N_2-1} \left(\max_{\hat{\xi}_2} |\hat{v}(., \hat{\xi}_2)|_{2,p,(0,1)} + \max_{\hat{\xi}_2} |\frac{\partial \hat{v}}{\partial \hat{\xi}_2}(., \hat{\xi}_2)|_{2,p,(0,1)} \right) \Bigg] \end{aligned} \tag{4.32}$$

where $|.|_{2,l,\hat{\mathbf{K}}}$ *and* $|.|_{2,p,(0,1)}$ *stand for the semi-norms associated with the spaces* $\mathrm{H}^k(\hat{\mathbf{K}})$ *and* $\mathrm{H}^p(0,1)$, *respectively.*

In the proof below, we need the following lemma (see [21], Thm. 3.13):

Lemma 4.9 (Bernstein inequality)**.** *If a trigonometric polynomial* $S(x)$ *of order* n *satisfies* $|S(x)| \leq M$ *for all* $x \in \mathbb{R}$, *then* $|S'(x)| \leq nM$. □

Proof of Lemma 4.8. First note that since $\hat{v} \in \mathrm{L}^2(0, 2\pi; \mathrm{H}^p((0,1)))$, the quantity $\|\hat{\mathbf{c}}_n\|_{\mathrm{H}^p(0,1)}$ is well defined. Using the triangular inequality, we have:

$$|\hat{v} - \hat{\Pi}_{\hat{\mathbf{K}}} \hat{v}|_{2,l,\hat{\mathbf{K}}} \leq |\hat{v} - T_{N_2}\hat{v}|_{2,l,\hat{\mathbf{K}}} + |T_{N_2}\hat{v} - \hat{\Pi}_{\hat{\mathbf{K}}} \hat{v}|_{2,l,\hat{\mathbf{K}}} \tag{4.33}$$

where, for every $0 \leq r \leq l$, we use the following notation:

$$T_{N_2}\left(\frac{\partial^r \hat{v}}{\partial \hat{\xi}_1^r}\right)(\hat{\xi}_1, \hat{\xi}_2) = \sum_{j=0}^{N_2} \frac{\partial^r \hat{v}}{\partial \hat{\xi}_1^r}\left(\hat{\xi}_1, \hat{\xi}_{2,j}\right) \hat{t}_j(\hat{\xi}_2) + \sum_{j=0}^{N_2} \frac{\partial^{r+1}\hat{v}}{\partial \hat{\xi}_1^r \partial \hat{\xi}_2}\left(\hat{\xi}_1, \hat{\xi}_{2,j}\right) \hat{s}_j(\hat{\xi}_2). \tag{4.34}$$

Observe that $\mathrm{H}^p(0,1) \hookrightarrow \mathrm{C}^k([0,1])$ and $T_{N_2}\left(\frac{\partial^r \hat{v}}{\partial \hat{\xi}_1^r}\right) = \frac{\partial^r}{\partial \hat{\xi}_1^r} \circ T_{N_2}\hat{v}$ for every $0 \leq r \leq l$. Thus, the terms in inequality (4.33) are well defined. Taking $\mathbf{X} = \mathrm{L}^2(0,1)$ and the function f as $\hat{\xi}_2 \to \frac{\partial^r \hat{v}}{\partial \hat{\xi}_1^r}(., \hat{\xi}_2)$ in Lemma 4.6, we obtain for $q \in \{0, 1, 2, \ldots\}$ such that $q + r \leq l$:

$$\left\| \frac{\partial^{q+r}\hat{v}}{\partial \hat{\xi}_1^r \partial \hat{\xi}_2^q} - \frac{\partial}{\partial \hat{\xi}_2^q} T_{N_2}\left(\frac{\partial^r \hat{v}}{\partial \hat{\xi}_1^r}\right) \right\|_{\mathrm{L}^\infty(0,2\pi;\mathbf{X})} \leq C(\hat{v}, b) q!\, (2(N_2+1))^q \frac{\coth^{q+1}(\frac{b}{2})}{\sinh^2(\frac{N_2+1}{2} b)} \tag{4.35}$$

where $C(\hat{v},b) = \left(\sum_{n=-\infty}^{\infty} \|\hat{\mathbf{c}}_n\|^2_{\mathrm{H}^p(0,1)} e^{2nb}\right)^{\frac{1}{2}}$ and $b > 0$ can be selected independently of r given the condition (4.43). Therefore, we deduce:

$$|\hat{v} - T_{N_2}\hat{v}|_{2,l,\hat{\mathbf{K}}} \leq \mathfrak{C}\left(\sum_{n=-\infty}^{\infty} \|\hat{\mathbf{c}}_n\|^2_{\mathrm{H}^p(0,1)} e^{2nb}\right)^{\frac{1}{2}} \frac{(N_2+1)^l}{\sinh^2(\frac{N_2+1}{2}b)}. \tag{4.36}$$

Now, we focus on the error estimate of $|T_{N_2}\hat{v} - \hat{\Pi}_{\hat{\mathbf{K}}}\hat{v}|_{2,l,\hat{\mathbf{K}}}$. Using (3.25) and the discussion in Section 3, we have:

$$\begin{aligned} T_{N_2}\hat{v} - \hat{\Pi}_{\hat{\mathbf{K}}}\hat{v} &= \sum_{j=0}^{N_2} \hat{v}\left(.,\hat{\xi}_{2,j}\right)\hat{t}_j + \sum_{j=0}^{N_2} \frac{\partial \hat{v}}{\partial \hat{\xi}_2}\left(.,\hat{\xi}_{2,j}\right)\hat{s}_j - \sum_{ij} \hat{\phi}_{ij}(\hat{v})\left[\hat{p}_i \otimes \hat{t}_j\right] - \sum_{ij} \hat{\psi}_{ij}(\hat{v})\left[\hat{p}_i \otimes \hat{s}_j\right] \\ &= \sum_{j=0}^{N_2}\left(\hat{v}(.,\hat{\xi}_{2,j}) - \sum_{i=0}^{k} \hat{p}_i^\star(\hat{v}(.,\hat{\xi}_{2,j}))\hat{p}_i\right)\hat{t}_j + \sum_{j=0}^{N_2}\left(\frac{\partial \hat{v}}{\partial \hat{\xi}_2}(.,\hat{\xi}_{2,j}) - \sum_{i=0}^{k} \hat{p}_i^\star(\frac{\partial \hat{v}}{\partial \hat{\xi}_2}(.,\hat{\xi}_{2,j}))\hat{p}_i\right)\hat{s}_j. \end{aligned} \tag{4.37}$$

Let r, q such that $r + q = l$, using Bernstein inequality in Lemma 4.9 and the fact that $\hat{t}_j \geq 0$ for every j, we have:

$$\begin{aligned} \left\|\frac{\partial^{q+r}}{\partial \hat{\xi}_1^r \partial \hat{\xi}_2^q}\left(T_{N_2}\hat{v} - \hat{\Pi}_{\hat{\mathbf{K}}}\hat{v}\right)\right\|_{\infty,\hat{\mathbf{K}}} &\leq N_2^q \left\|\frac{\partial^r}{\partial \hat{\xi}_1^r}\left(T_{N_2}\hat{v} - \hat{\Pi}_{\hat{\mathbf{K}}}\hat{v}\right)\right\|_{\infty,\hat{\mathbf{K}}} \\ &\leq N_2^q \max_{\hat{\xi}_2} \sum_{j=0}^{N_2}\left|\hat{v}(.,\hat{\xi}_{2,j}) - \sum_{i=0}^{k} \hat{p}_i^\star(\hat{v}(.,\hat{\xi}_{2,j}))\hat{p}_i\right|_{\infty,r,(0,1)} \hat{t}_j + \\ &\quad N_2^q \max_{\hat{\xi}_2}\left|\sum_{j=0}^{N_2}\left|\frac{\partial \hat{v}}{\partial \hat{\xi}_2}(.,\hat{\xi}_{2,j}) - \sum_{i=0}^{k} \hat{p}_i^\star(\frac{\partial \hat{v}}{\partial \hat{\xi}_2}(.,\hat{\xi}_{2,j}))\hat{p}_i|_{\infty,r,(0,1)}\right|\hat{s}_j\right| \end{aligned} \tag{4.38}$$

where $|.|_{\infty,r,(0,1)}$ stands for the semi-norm related to the space $\mathrm{W}^{\infty,l}(0,1)$. Using the identity (3.21) for $\hat{t}_j$ and the inequality $\max_{\hat{\xi}_2}|\hat{s}| \leq \frac{2}{N_2+1}$, we deduce:

$$\begin{aligned} \left\|\frac{\partial^{q+r}}{\partial \hat{\xi}_1^r \partial \hat{\xi}_2^q}\left(T_{N_2}\hat{v} - \hat{\Pi}_{\hat{\mathbf{K}}}\hat{v}\right)\right\|_{\infty,\hat{\mathbf{K}}} &\leq 2N_2^q\left(\max_j|\hat{v}(.,\hat{\xi}_{2,j}) - \sum_{i=0}^{k} \hat{p}_i^\star(\hat{v}(.,\hat{\xi}_{2,j}))\hat{p}_i|_{\infty,r,(0,1)} + \right. \\ &\quad \left. \max_j|\frac{\partial \hat{v}}{\partial \hat{\xi}_2}(.,\hat{\xi}_{2,j}) - \sum_{i=0}^{k} \hat{p}_i^\star(\frac{\partial \hat{v}}{\partial \hat{\xi}_2}(.,\hat{\xi}_{2,j}))\hat{p}_i|_{\infty,r,(0,1)}\right). \end{aligned} \tag{4.39}$$

Next, we need the following claim: If $\hat{w} \in \mathrm{C}^k([0,1])$, then, for every $0 \leq r \leq l$:

$$|\hat{w} - \sum_{i=0}^{k} \hat{p}_i^\star(\hat{w})\hat{p}_i|_{\infty,r,(0,1)} \leq \mathfrak{C}|\hat{w}|_{2,p,(0,1)}. \tag{4.40}$$

Indeed, by virtue of (3.24), it is not difficult to see:

$$|\hat{w} - \sum_{i=0}^{k} \hat{p}_i^\star(\hat{w})\hat{p}_i|_{\infty,r,(0,1)} \leq \mathfrak{C}\|\hat{w}\|_{\mathrm{C}^r([0,1])}. \tag{4.41}$$

Since $\mathrm{H}^p(0,1) \hookrightarrow \mathrm{C}^k([0,1])$, applying Theorem 3.1.1 in [7], we get (4.40). As a consequence, we obtain:

$$|T_{N_2}\hat{v} - \hat{\Pi}_{\hat{\mathbf{K}}}\hat{v}|_{\infty,l,\hat{\mathbf{K}}} \leq \mathfrak{C}\,\frac{N_2^{l+1}-1}{N_2-1}\left(\max_{\hat{\xi}_2}|\hat{v}(.,\hat{\xi}_2)|_{2,p,(0,1)} + \max_{\hat{\xi}_2}|\frac{\partial \hat{v}}{\partial \hat{\xi}_2}(.,\hat{\xi}_2)|_{2,p,(0,1)}\right). \tag{4.42}$$

The proof is complete. □

Corollary 4.10. *Consider the reference finite element* $\left(\mathbf{K}, \mathbf{P}_{\mathbf{K}}^{[k,N_2]}, \mathbf{T}_{\mathbf{K}}^{\star}\right)$ *with* $N_2 \geq 2$. *Let* p *and* m *some positive integers with* $k \leq m < p$ *and* v *is a function defined on* $\mathbf{K}$ *such that:*

(1) $h = |\xi_{1,0} - \xi_{1,1}| < R$
(2) $v \in \mathrm{L}^2(0, 2\pi R; \mathrm{H}^p(\xi_{1,0}, \xi_{1,1}))$, *i.e.,* $v(., \xi_2) \in \mathrm{H}^p(\xi_{1,0}, \xi_{1,1})$ *a.e.*
(3) If $\mathbf{c}_n = \frac{1}{2\pi R}\int_0^{2\pi R} v(., \xi_2) e^{-i_c \frac{n\xi_2}{R}}\, d\xi_2$, *we have:*

$$0 \leq \limsup_n \sqrt[n]{\|\mathbf{c}_n\|_{\mathrm{H}^p(\xi_{1,0},\xi_{1,1})}} < 1 \tag{4.43}$$

then, for sufficiently small h, *there exists* $b > 0$ *such that for every* $0 \leq l \leq k$:

$$\begin{aligned} |v - \Pi_{\mathbf{K}} v|_{2,l,\mathbf{K}} \leq \mathfrak{C} \Bigg[\left(\sum_{n=-\infty}^{\infty} \|\mathbf{c}_n\|^2_{\mathrm{H}^p(\xi_{1,0},\xi_{1,1})} e^{2nb} \right)^{\frac{1}{2}} \frac{(N_2+1)^l}{h^l \sinh^2\left(\frac{N_2+1}{2} b\right)} + \\ h^{p-l} \frac{N_2^{l+1}-1}{N_2-1} \|v\|_{\mathrm{H}^2(0,2\pi R;\mathrm{H}^p(\xi_{1,0},\xi_{1,1}))} \Bigg] \end{aligned} \tag{4.44}$$

Proof. Indeed, since $h < R$ and using $\hat{v} = v \circ \mathbf{F}_{\mathbf{K}}$, we obtain:

$$|v - \Pi_{\mathbf{K}} v|_{2,l,\mathbf{K}} \leq \frac{meas(\mathbf{K})^{\frac{1}{2}}}{h^l} |\hat{v} - \hat{\Pi}_{\hat{\mathbf{K}}} \hat{v}|_{2,l,\hat{\mathbf{K}}} \tag{4.45}$$

where $meas(\mathbf{K})$ denotes the Lebesgue measure of $\mathbf{K}$. Since the assumptions of Lemma 4.8 are satisfied, combining (4.32) with the following inequalities:

$$\begin{cases} \max\limits_{\hat{\xi}_2} |\hat{v}(., \hat{\xi}_2)|_{2,p,(0,1)} \leq \mathfrak{C} \frac{h^p}{meas(\mathbf{K})^{\frac{1}{2}}} \|v\|_{\mathrm{H}^2(0,2\pi R;\mathrm{H}^p(\xi_{1,0},\xi_{1,1}))} \\ \max\limits_{\hat{\xi}_2} |\frac{\partial \hat{v}}{\partial \hat{\xi}_2}(., \hat{\xi}_2)|_{2,p,(0,1)} \leq \mathfrak{C} \frac{h^p}{meas(\mathbf{K})^{\frac{1}{2}}} \|v\|_{\mathrm{H}^2(0,2\pi R;\mathrm{H}^p(\xi_{1,0},\xi_{1,1}))} \\ \|\hat{\mathbf{c}}_n\|_{\mathrm{H}^p(0,1)} \leq \mathfrak{C} \frac{1}{meas(\mathbf{K})^{\frac{1}{2}}} \|\mathbf{c}_n\|_{\mathrm{H}^p(\xi_{1,0},\xi_{1,1})} \end{cases} \tag{4.46}$$

The result follows immediately.

□

Proof of Theorem 4.4. By Céa Lemma, we have:

$$\|\mathbf{u} - \mathbf{u}_h\|_{\mathbf{V_h}(\Sigma)} \leq \mathfrak{C} \inf_{\mathbf{w}_h \in \mathbf{V_h}(\Sigma)} \|\mathbf{u} - \mathbf{w}_h\|. \tag{4.47}$$

To proceed let us define $\mathbf{w}_h = (w_{l,h})_{1 \leq l \leq 3}$ such that:

$$\mathbf{w}_h = \mathbf{w}_h^{(1)} - \mathbf{w}_h^{(2)}. \tag{4.48}$$

Here, $\mathbf{w}_h^{(1)} = (w_{l,h}^{(1)})_{1 \leq l \leq 3}$ and $\mathbf{w}_h^{(2)} = (w_{l,h}^{(2)})_{1 \leq l \leq 3}$, where for each element $\mathbf{K}_m$ $(1 \leq m \leq N_1)$:

$$\begin{aligned} w_{l,h}^{(1)} &= \Pi_h u_l \\ w_{l,h}^{(2)}|_{\mathbf{K}_m} &= \sum_{ij} \psi_{ij}^{l,m} \left(u_l|_{\mathbf{K}_m} \right) p_i^{l,m} \otimes s_{N_2} \end{aligned} \tag{4.49}$$

where the linear forms $\psi_{ij}^{l,m}$ are associated with $\left(\mathbf{K}_m, \mathbf{P}_{\mathbf{K}_m}^{[k_l,N_2]}, \ \mathbf{T}_{\mathbf{K}_m}^{\star}\right)$. Observe that $w_{l,h}|_{\mathbf{K}_m} \in \mathbf{P}_{\mathbf{K}_m}^{[k_l,N_2]}$, for every $1 \leq l \leq 3$, as a consequence of (3.18). Furthermore, under the assumption $(\mathbf{H}_\Pi)$ and the assumption (5), we have:

$$\mathbf{w}_h^{(1)} \in \mathbf{V_h}. \tag{4.50}$$

The next step is to show that $\mathbf{w}_h^{(2)} \in \mathbf{V_h}$. To do this, we first establish that $\mathbf{w}_h^{(2)} \in \mathrm{H}^1(\Sigma) \times \mathrm{H}^1(\Sigma) \times \mathrm{H}^2(\Sigma)$. Focusing on the component $l = 1$ and using Theorem 2.1.4 in [20] and the fact that $w_{1,h}^{(1)} \in \mathrm{H}^1(\Sigma)$, we deduce:

$$\sum_{i=0}^{k} \psi_{ij}^{l,m}\left(u_l|_{\mathbf{K}_m}\right) p_i^{l,m}(\xi_{1,m}) = \sum_{i=0}^{k} \psi_{ij}^{l,m+1}\left(u_l|_{\mathbf{K}_{m+1}}\right) p_i^{l,m+1}(\xi_{1,m}) \tag{4.51}$$

which holds for adjacent elements $\mathbf{K}_m$ and $\mathbf{K}_{m+1}$, with $1 \leq m < N_1$. Using again Theorem 2.1.4 in [20], we conclude that $w_{1,h}^{(2)} \in \mathrm{H}^1(\Sigma)$. Similar arguments apply for $l = 2$. For $l = 3$, the argument is repeated for both $w_{3,h}^{(1)}$ and $\nabla w_{3,h}^{(1)}$.

Next, we show that $\mathbf{T}\mathbf{w}_h^{(2)} = 0$ on Γ_0. Let us assume that an element $\mathbf{K}_m$ exists such that $\partial(\mathbf{K}_m \times [-\frac{e}{2}, \frac{e}{2}]) \cap \Gamma_0 \neq \emptyset$. From the definition of Γ_0, we should consider four cases:

i- $\partial(\mathbf{K}_m \times [-\frac{e}{2}, \frac{e}{2}]) \cap \Gamma_0 \cap (0, L) \times (0, 2\pi R) \times \{\frac{e}{2}\} \neq \emptyset$
ii- $\partial(\mathbf{K}_m \times [-\frac{e}{2}, \frac{e}{2}]) \cap \Gamma_0 \cap (0, L) \times (0, 2\pi R) \times \{-\frac{e}{2}\} \neq \emptyset$
iii- $\partial(\mathbf{K}_m \times [-\frac{e}{2}, \frac{e}{2}]) \cap \Gamma_0 \cap \{0\} \times (0, 2\pi R) \times [-\frac{e}{2}, \frac{e}{2}] \neq \emptyset$
iv- $\partial(\mathbf{K}_m \times [-\frac{e}{2}, \frac{e}{2}]) \cap \Gamma_0 \cap \{L\} \times (0, 2\pi R) \times [-\frac{e}{2}, \frac{e}{2}] \neq \emptyset$

Here, we detail cases i and iii since analogous arguments apply to cases ii and iv.

Case i: taking into account $\mathbf{T}\mathbf{w}_h^{(1)} = 0$ on Γ_0 and the displacement field- expression (2.8) together with the fact that we are dealing with polynomials, we have:

$$w_{3,h}^{(2)}|_{\mathbf{K}_m} = 0. \tag{4.52}$$

Combining with (2.8) and (2.12), we obtain:

$$w_{1,h}^{(2)}|_{\mathbf{K}_m} = w_{2,h}^{(2)}|_{\mathbf{K}_m} = 0. \tag{4.53}$$

Obviously, we deduce $\mathbf{T}\mathbf{w}_h^{(2)} = 0$ on $\partial(\mathbf{K}_m \times [-\frac{e}{2}, \frac{e}{2}]) \cap \Gamma_0 \cap (0, L) \times (0, 2\pi R) \times \{\frac{e}{2}\}$.

Case iii: we note that this corresponds to the first element, *i.e.*, $m = 1$. Using the fact that $\mathbf{T}\mathbf{w}_h^{(1)} = 0$ on Γ_0 and the displacement field expression (2.8), we deduce:

$$w_{1,h}^{(1)}|_{\mathbf{K}_1}(\xi_1 = 0, \xi_2) = w_{2,h}^{(1)}|_{\mathbf{K}_1}(\xi_1 = 0, \xi_2) = w_{3,h}^{(1)}|_{\mathbf{K}_1}(\xi_1 = 0, \xi_2) = 0 \quad \forall\, \xi_2 \in [0, 2\pi R]. \tag{4.54}$$

This particulary implies for every j:

$$\sum_{i=0}^{k} \psi_{ij}^{l,1}\left(u_l|_{\mathbf{K}_1}\right) p_i^{l,1}(\xi_1 = 0) = 0 \quad 1 \leq l \leq 3. \tag{4.55}$$

Consequently, using (4.49) we deduce $\mathbf{T}\mathbf{w}_h^{(2)} = 0$ on $\partial(\mathbf{K}_1 \times [-\frac{e}{2}, \frac{e}{2}]) \cap \Gamma_0 \cap \{0\} \times (0, 2)\pi R) \times [-\frac{e}{2}, \frac{e}{2}]$.

In the subsequent, we focus on the error estimates considering the component $l = 1$ for simplicity. Using Corollary 4.10 and the fact that $p > 1$, we deduce the existence of a constant $b_1 > 0$ such that for sufficiently small $h_{\max}$:

$$\begin{aligned} \|u_1 - \Pi_h u_1\|_{\mathrm{H}^1(\Sigma)} \leq \mathfrak{C} \Bigg[& \left(\sum_{n=-\infty}^{\infty} \|\mathbf{c}_{1,n}\|^2_{\mathrm{H}^{p_1}(0,L)} e^{2nb_1} \right)^{\frac{1}{2}} \frac{N_2+1}{h_{\min} \sinh^2\left(\frac{N_2+1}{2} b_1\right)} + \\ & h_{\max}^{p_1-1} \frac{N_2^2-1}{N_2-1} \|u_1\|_{\mathrm{H}^2(0,2\pi R;\mathrm{H}^{p_1}(0,L))} \Bigg]. \end{aligned} \tag{4.56}$$

Moreover, Lemma 4.7 implies:

$$\begin{aligned}\|w_{1,h}^{(2)}\|^2_{\mathrm{H}^1(\Sigma)} &\leq \sum_m \frac{meas(\mathbf{K}_m)}{h^2_{\min}} \|\sum_{ij} \hat{\psi}_{ij}^{l,m}(\hat{u}_1)\hat{p}_i^{(1)} \otimes \hat{s}_{N_2}\|^2_{\mathrm{H}^1(\hat{\mathbf{K}}_m)} \\ &\leq \mathfrak{C} \sum_m \sum_i \frac{meas(\mathbf{K}_m)}{h^2_{\min}} \frac{1}{N_2^{2(r-l_i-1)}} \|(N_2+1)\hat{p}_i^{(1)} \otimes \hat{s}_{N_2}\|^2_{\mathrm{H}^1(\hat{\mathbf{K}}_m)} \\ &\leq \mathfrak{C} \sum_m \sum_i \frac{N_2^2}{h^2_{\min}} \frac{meas(\mathbf{K}_m)}{N_2^{2(r-l_i-1)}} \\ &\leq \mathfrak{C} \frac{N_2^2}{h^2_{\min}} \frac{1}{N_2^{2(r-k_1-1)}}\end{aligned} \tag{4.57}$$

for every integer $r \geq \max_{1\leq i\leq 3}\{m_i\}$. In the second line we have used the fact that $\|\frac{\partial^r \hat{u}_1}{\partial \hat{\xi}_1^j \partial \hat{\xi}_2^{r-j}}\|_{\infty,\hat{\mathbf{K}}_m} \leq \mathfrak{C}\|\frac{\partial^r u_1}{\partial \xi_1^j \partial \xi_2^{r-j}}\|_{\infty,\mathbf{K}_m}$ for $0 \leq j \leq l_i$ and for sufficiently small $h_{\max}$. In the third line of (4.57), we have used the Bernstein inequality in Lemma 4.9 as well as the inequality $\max_{\hat{\xi}_2}|\hat{s}_{N_2}| \leq \frac{2}{N_2+1}$. The proof of the case $l = 2$ follows exactly the same arguments as the previous case, maybe with different constant $b_2 > 0$. The proof of the remaining case $l = 3$ is only a minor change of the previous one and we finally get:

$$\begin{aligned}\|u_3 - u_{3,h}\|_{\mathrm{H}^2(\Sigma)} \leq \mathfrak{C} \Bigg[\left(\sum_{n=-\infty}^{\infty} \|\mathbf{c}_{3,n}\|^2_{\mathrm{H}^{p_3}(0,L)} e^{2nb_3} \right)^{\frac{1}{2}} \frac{(N_2+1)^2}{h^2_{\min}\sinh^2\left(\frac{N_2+1}{2}b_3\right)} + \\ h_{\max}^{p_3-2}\frac{N_2^3-1}{N_2-1}\|u_3\|_{\mathrm{H}^2(0,2\pi R;\mathrm{H}^{p_3}(0,L))} + \frac{N_2^2}{h^2_{\min}}\frac{1}{N_2^{r-k_3-1}}\Bigg].\end{aligned} \tag{4.58}$$

This completes the proof. □

5. Numerical examples

In this section, we present three sample analyses involving elastic pipes. The first two examples involve a straight pipe, while the final example is focused on a curved pipe. It is worth highlighting that the 3D plots associated with the current pipe element were generated using an additional set of points and the interpolation relations outlined in Definition 3.5, due to the relatively small value of the parameter N_2.

For comparison purposes, additional computations are performed using shell elements and a Fourier-based pipe element, known as ELBOW31, available in Abaqus software. It is worth noting that the employed shell elements are four-nodes, identified as S4R5 in Abaqus software, and characterized by six degrees of freedom per node that uses bilinear interpolation and reduced integration [14]. The present pipe element used in the examples below is equivalent to ELBOW31 in terms of interpolation orders, except that the latter is limited to 6 Fourier modes.

In terms of numerical integration, the quadratic Gauss method is employed along the ξ_1 and ξ_3 directions using 2 points, while the Gauss-Chebyshev scheme is applied along the ξ_2 direction with $2N_2 + 1$ points. This approach ensures the achievement of, at least, an exact integration for straight pipes, according to Lemma 3.3.

5.1. Straight pipe under compression load

This first example deals with a straight pipe, *i.e.*, $\kappa = 0$, clamped at one extremity and subjected to the traction or the compression load applied at the other extremity as depicted in Figure. The pipe characteristics are summarized in Table 1.

The numerical solutions are computed in the space $\mathbf{P}_{\mathbf{K}}^{[1,N_2]} \times \mathbf{P}_{\mathbf{K}}^{[1,N_2]} \times \mathbf{P}_{\mathbf{K}}^{[3,N_2]}$, where the basis of $\mathbb{P}_1$ and $\mathbb{P}_3$, given in Example 3.2, are used. The parameter N_2 is chosen to be variable with an uniform discretization along ξ_1, *i.e.*, $h = h_{\max} = h_{\min}$ such that $\frac{2\pi R}{N_2}$ has the same order of magnitude as h. An imposed total load P with magnitude 30000 is applied .

According to Figure 5, it can be observed that the radial displacement isovalues for the new pipe element are in good agreement with the results obtained using the shell elements. Picking out a point M at the middle of the

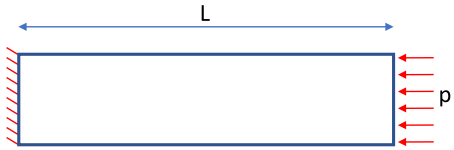

FIGURE 4. Straight pipe with radius R subjected to compression load.

TABLE 1. Material and geometric properties of the straight pipe.

L	R	e	E	ν
5	0.5	0.01	10^9	0.3

TABLE 2. Relative error err_{disp} related to the new pipe element for different value of N_2.

N_2	h	$ndofs$	$u_{3,h}(\frac{L}{2})$	$u_{3,ref}$	err_{disp}
1	1.25	100	1.45107e-4	1.432394e-4	1.3e-2
3	0.833	252	1.43530e-4	1.432394e-4	2e-3
6	0.41	780	1.43234e-4	1.432394e-4	3.6e-5
11	0.25	2100	1.43235e-4	1.432394e-4	3.1e-5

TABLE 3. Relative error err_{disp} related to ELBOW31 element for different value of N_2.

N_2	h	$ndofs$	$u_{3,h}(\frac{L}{2})$	$u_{3,\text{ref}}$	err_{disp}
1	1.25	60	1.44671e-4	1.432394e-4	1e-2
3	0.833	196	1.43339e-4	1.432394e-4	7e-4
6	0.41	676	1.43253e-4	1.432394e-4	1e-4

mid-surface, the numerical radial displacements $u_{3,h}(M)$, associated with the new pipe element, are compared in Table 2 against the following analytical value $u_{3,ref}$:

$$u_{3,ref} = -\frac{\nu}{E}\frac{P}{2\pi e}. \tag{5.1}$$

In Table 2, $ndofs$ and err_{disp} stand for the total number of degrees of freedom and the relative error $\frac{|u_{3,h}(\frac{L}{2})-u_{3,ref}|}{|u_{3,ref}|}$, respectively. It is seen that the relative error remains small, *i.e.*, less than 3.5e-3, and the accuracy improves as the parameter N_2 increases. It is also noteworthy that good results are obtained even for small values of the parameter N_2, which corresponds to $N_2 + 1$ points at each pipe section. This may be due to the fact that only the first ovalization mode is activated in this case, as the displacement is uniform in the radial direction.

Furthermore, analogous results for the ELBOW31 element, introduced at the beginning of this part, are presented in Table 3. It is seen that the radial displacement is quite close to the reference value with a small error. The computation using the shell element with a fine mesh, *i.e.*, mesh size equal to 0.05, also yileds a close value equal to 1.432e-4.

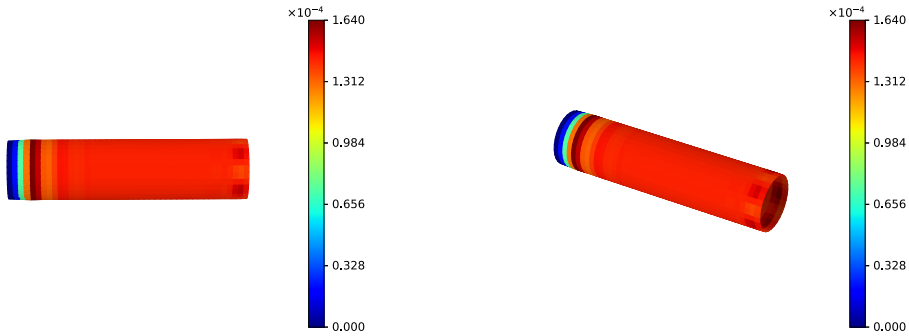

(a)

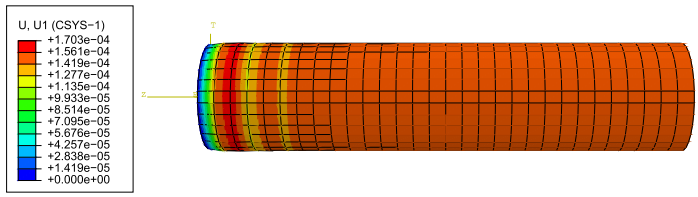

(b)

FIGURE 5. Radial displacement ($u_{3,h}$) isovalues using the new pipe element ($N_2 = 3$) (a) and shell elements (b).

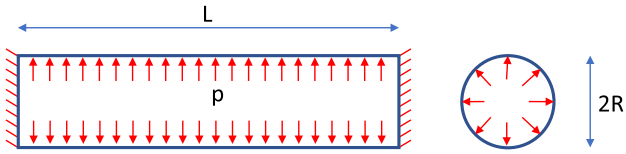

FIGURE 6. Straight pipe with radius R subjected to internal pressure p.

5.2. Straight pipe under internal pressure

In this example, we use the same straight pipe with the same properties and solution spaces as in the previous example, which is subjected to an uniform internal pressure $p = 30000$ while both extremities are clamped (see Fig. 6). The radial displacement isovalues obtained using the new pipe element and the 4-node shell element are compared in Figure 7, which shows a good agreement between the results

Similarly, the radial displacement associated with a point picked at the mid-surface in the middle of the pipe and compared in Table 4 to the one computed using the shell elements and the following analytical solution:

$$u_{3,ref} = \frac{A}{E}(1-\nu)(1-2\nu)(R+\xi_3) + \frac{B}{E}(1+\nu)\frac{1}{(R+\xi_3)} \tag{5.2}$$

where $A = p\frac{(R-\frac{e}{2})^2}{2Re}$ and $B = p\frac{(R-\frac{e}{2})^2(R+\frac{e}{2})^2}{2Re}$. These variables, along equation (5.2), are obtained using three-dimensional elasticity theory while omitting the boundary conditions. The results associated with the shell element have been computed using a sufficiently fine mesh, *i.e.*, 38178 degrees of freedom, in order to avoid the spurious effects of the mesh size. Tables 4 and 5 summarise an overview of the relative errors computed

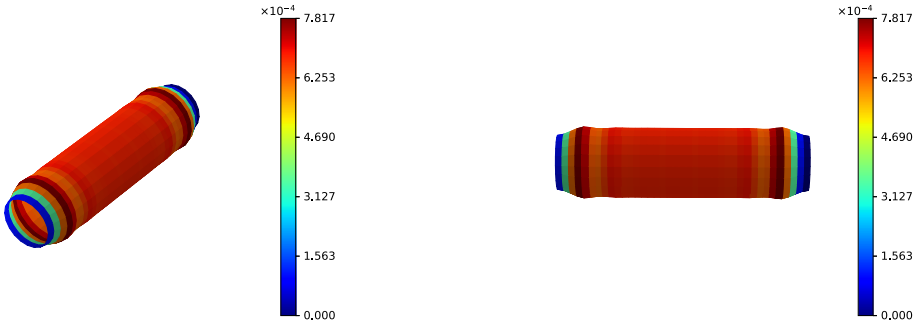

(a)

(b)

FIGURE 7. Radial displacement ($u_{3,h}$) isovalues using the new pipe element ($N_2 = 3$) (a) and shell elements (b).

for the present pipe element and the ELBOW31 element, respectively. Regarding the new element, it is seen that an enhanced accuracy is achieved as the number of nodes increases (at least 5 nodes per finite element section). Similar results are also obtained for ELBOW31 element, where the relative error remains consistently small. Finally, the computation using the shell elements yields a displacement value of 6.8e-4, consistent with the previous computations.

Figure 8 displays the plot of the relative energy error $\sqrt{\frac{a(\mathbf{u}-\mathbf{u_h},\mathbf{u}-\mathbf{u_h})}{a(\mathbf{u},\mathbf{u})}}$ that the error decreases as the parameter N_2 increases, indicating a convergence of the numerical solution to the analytical expression (5.2) even if the latter was obtained within the framework of three dimensional elasticity. Notably, there exists an equivalence between the aforementioned relative error and the relative error expressed in terms of the norm $\|\|_{\mathbf{V}_h}$, *i.e.*, $\frac{\|\mathbf{u}-\mathbf{u_h}\|_{\mathbf{V}_h}}{\|\mathbf{u}\|_{\mathbf{V}_h}}$, using Lemma 2.1.

Now, we are considering a more complex loading scenario with a non-uniform internal pressure described by the equation $p = 1000\cosh\left(\cos\left(\frac{\xi_2}{R}\right)\right)$. The boundary conditions for this case are the same as before, with both extremities fixed. Since there is no analytical solution for this particular case, we will compare the results obtained using shell elements. To avoid the effect of mesh size, we have used sufficiently dense mesh in the case of shell elements, *i.e.*, mesh size equal to 0.02 equivalent to 236442 degrees of freedom. Qualitatively, the plots in Figure 9 show that the deformed shape obtained using the new pipe element with $N_2 = 5$ is similar to that obtained using the shell elements. Quantitatively, Table 6 summarizes the relative error in the radial displacement at the point $M = \left(\frac{L}{2}, 0\right)$ computed using the new pipe element and compared to the corresponding shell element results as the reference result.

In this complex case, it is seen that the radial displacement obtained using the current pipe elements is relatively closer to the reference result. Moreover, the results obtained in Table 6, using different values of the parameter N_2, remain relatively close to each other, even for a smaller number of degrees of freedom, *i.e.*, less than 520 degrees of freedom.

TABLE 4. Relative error err_{disp} related to the new pipe element for different value of N_2.

N_2	h	$ndofs$	$u_{3,h}(M)$	$u_{3,ref}$	err_{disp}
1	1.5	80	6.99e-4	6.78e-4	3.1e-2
3	0.833	252	6.88e-4	6.78e-4	1e-2
5	0.55	520	6.80e-4	6.78e-4	3e-3
15	0.2	3432	6.76e-4	6.78e-4	2.9e-3
25	0.12	8904	6.77e-4	6.78e-4	1.4e-3

TABLE 5. Relative error err_{disp} related to ELBOW31 element for different value of N_2.

N_2	h	$ndofs$	$u_{3,h}(M)$	$u_{3,ref}$	err_{disp}
1	1.5	48	6.91e-4	6.78e-4	2e-2
3	0.833	196	6.84e-4	6.78e-4	9e-3
5	0.55	440	6.82e-4	6.78e-4	7e-3

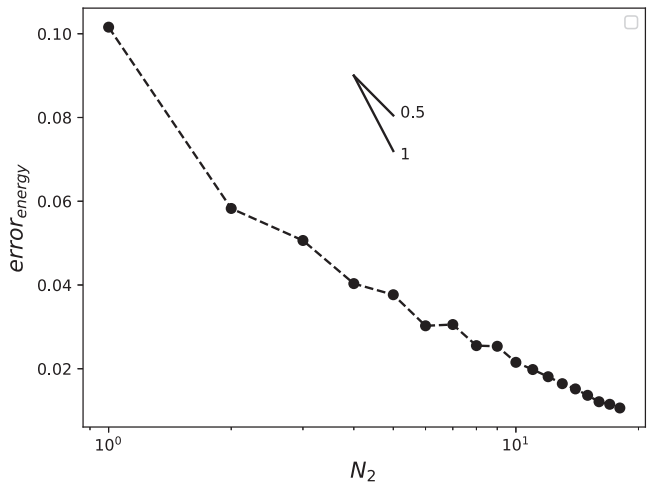

FIGURE 8. Relative energy error with respect to N_2.

Finally and for comparison purposes, the relative errors, related to the shell elements, are displayed in Table 7 for different values of mesh sizes, with the reference result being the same as for pipe elements. Is is noteworthy that employing a mesh size exceeding 0.4 for shell elements leads to an error greater than 20%, which is comparatively higher than using the new pipe element with a lower number of degrees of freedom.

5.3. Elbow under internal pressure

In this example, the focus is on studying the impact of curvature on the behavior of an elbow part under constant internal pressure. The elbow part used has a curvature of $\kappa = \frac{1}{R_c} = \frac{1}{3}$, and both of its ends are fixed. The applied pressure is equal to 30000. The properties of the elbow part, aside from its curvature, are the same as those used in previous examples. The elbow problem is depicted in Figure 10.

The magnitude of the displacement for the new pipe element and the shell elements is depicted in Figure 11 for the case where $N_2 = 7$. Both methods produce deformed shapes that are in good agreement and show

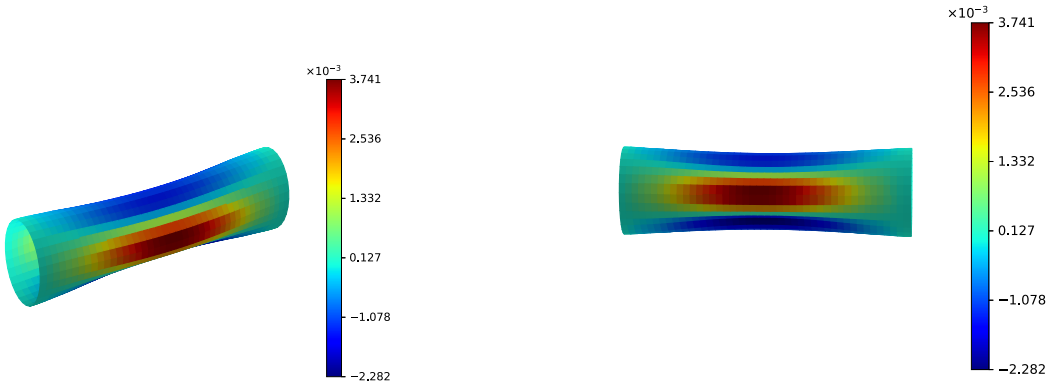

(a)

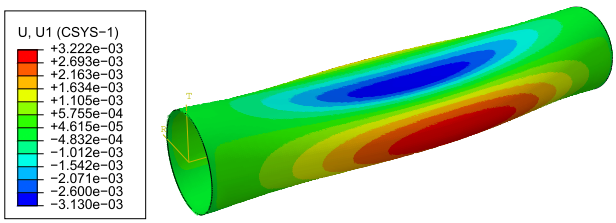

(b)

FIGURE 9. Radial displacement ($u_{3,h}$) isovalues using the new pipe element ($N_2 = 5$) (a) and the shell elements (b).

TABLE 6. Relative errors err_{disp} of the radial displacement at the point M with respect to the shell elements (new pipe element).

N_2	h	$ndofs$	$u_{3,h}(M)$	err_{disp}
1	1.5	80	4e-5	0.99
3	0.833	252	2.84e-3	1.1e-1
5	0.55	520	3.66e-3	1.3e-1
15	0.2	3432	3.95e-3	2.2e-1
25	0.12	8904	3.78e-3	1.7e-1
30	0.102	12600	3.74e-3	1.6e-1

TABLE 7. Relative errors err_{disp} of the radial displacement at the point M for shell elements using different mesh sizes.

h	$ndofs$	$u_{3,h}(M)$	err_{disp}
0.5	396	2.3e-3	3e-1
0.4	672	2.6e-3	2e-1
0.2	3000	2.9e-3	1e-1

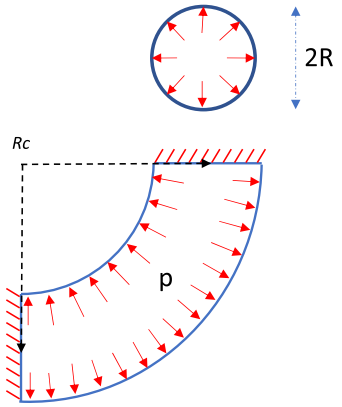

FIGURE 10. Elbow with curvature $\kappa = \frac{1}{R_c}$ subjected to uniform internal pressure p.

TABLE 8. Relative errors err_{dis} of the displacement magnitude at the point M with respect to the shell elements.

N_2	h	$ndofs$	$u_h(M)$	err_{disp}
3	0.78	252	2.430e-3	6e-3
7	0.39	884	2.4032e-3	5e-3
11	0.2	1900	2.489e-3	3e-2
25	0.12	8692	2.519e-3	4e-2
30	0.101	11844	2.507e-3	3.8e-2
35	0.087	16060	2.497e-3	3.3e-2

non-uniform ovalization along the elbow axis, which is different from the uniform ovalization observed in the straight pipe in the previous example. The maximal values of the displacement magnitude for both methods are similar and are of the order of 2e-3. The previous results obtained using the new pipe element were computed using 512 degrees of freedom.

Finally, Table 8 shows the relative errors (with respect to the shells results) of the displacement magnitude, denoted u_h, associated with the point $(0, \frac{L}{2})$ in the curvilinear coordinates. The 3D computation using the shell elements, with a mesh size equal to 0.05, gives a value of 2.41e-3. It is seen that the computed errors are relatively small even for low values of the parameter N_2.

These results show again the capabilities of the present pipe element to capture the three dimensional shell behaviour for curved parts with less computational cost compared with shell elements computations. Indeed, in the context of shell elements, using 600 degrees of freedom would be equivalent to using a mesh size approximately equal to 0.4 which is considered as a very coarse mesh take into account the geometric characteristics of the model. Moreover, the relative errors err_{disp} associated with the shell elements and computed using different coarse mesh sizes, as shown in Table 9, show again that the relative errors are important compared to the new pipe elements for equivalent number of degrees of freedom.

6. CONCLUSIONS

In this paper, a new pipe finite element for analyzing the behavior of pipes has been introduced within the framework of linear shell theory. This element is based on the use of Hermite-Jackson trigonometric interpolation along the contour of each section of the pipe and classical polynomial interpolation along the pipe axis in

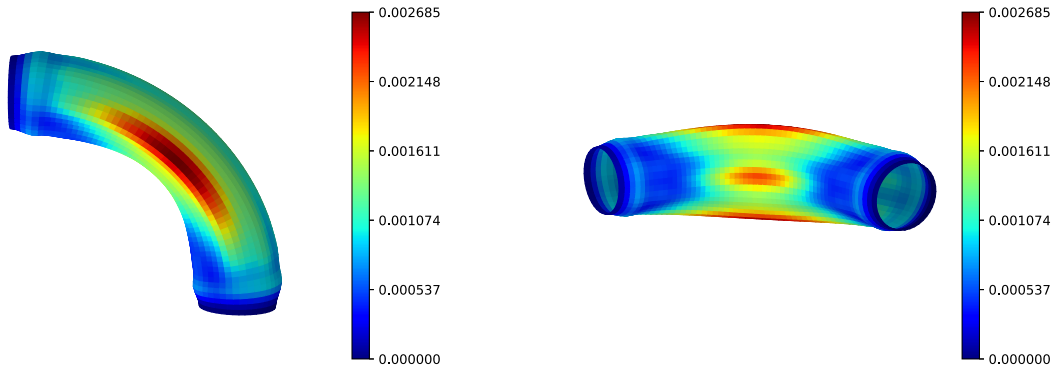

(a)

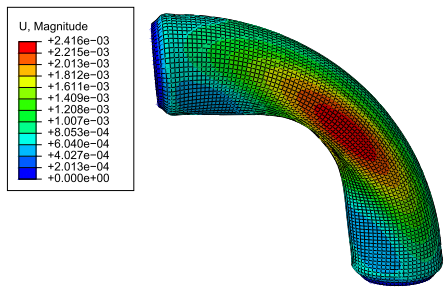

(b)

FIGURE 11. Displacement magnitude isovalues using the new pipe element ($N_2 = 7$) (a) and the shell elements (b).

TABLE 9. Relative errors err_{disp} of the radial displacement at the point M for shell elements.

h	$ndofs$	$u_h(M)$	err_{disp}
0.5	360	1.3e-3	4.5e-1
0.4	624	1.9e-3	2e-1
0.25	1638	2e-3	1.6e-1

curvilinear coordinates. The numerical solution is obtained using a mixed strategy that incorporates Lagrange multipliers to impose the constraints associated with the new pipe element, along with the application of Dirichlet boundary conditions. The error estimates for this element, under specific assumptions on the exact solution, show that the numerical solution converges as long as the step size along the pipe axis is of the same order as the one along the section contour. Moreover, the comparison with shell elements show that the computational cost is quite equivalent to that of coarse shell models. In the light of the achieved results, several promising topics for future research may be investigated. Firstly, while the current work focused on the development and analysis of the new pipe element, extending its applicability to more complex cases involving fluid-structure interaction problems would be of significant value. Additionally, an in-depth investigation of locking issues encountered in shell modeling could provide valuable insights for these particular types of finite elements.

References

[1] W. Arendt and S. Bu, Fourier series in banach spaces and maximal regularity. In: *Vector Measures, Integration and Related Topics*. Birkhäuser, Basel (2009) 21–39.

[2] K.J. Bathe and C.A. Almeida, A simple and effective pipe elbow element—linear analysis. *J. Appl. Mech.* **47** (1980) 93–100.

[3] K.J. Bathe and C.A. Almeida, A simple and effective pipe elbow element—interaction effects. *J. Appl. Mech.* **49** (1982) 165–171.

[4] K.-J. Bathe, C.A. Almeida and L.W. Ho, A simple and effective pipe elbow element—some nonlinear capabilities. In: *Nonlinear Finite Element Analysis and Adina*. Elsevier (1983) 659–667.

[5] D. Chapelle and K.-J. Bathe, The Finite Element Analysis of Shells - Fundamentals. Springer, Berlin, Heidelberg (2011).

[6] P.G. Ciarlet, Theory of shells: Volume 3. Studies in mathematics and its applications. North-Holland, Oxford, England (2000).

[7] P.G. Ciarlet, The Finite Element Method for Elliptic Problems. Society for Industrial and Applied Mathematics (2002).

[8] C. Farhat and F. Roux, A method of finite element tearing and interconnecting and its parallel solution algorithm. *Int. J. Numer. Methods Eng.* **32** (1991) 1205–1227.

[9] L. Grafakos, Classical Fourier Analysis. Springer, New York (2014).

[10] S. Hu and N.S. Papageorgiou, Handbook of Multivalued Analysis. Springer, US (2000).

[11] D. Jackson, A formula of trigonometric interpolation. *Rend. Circ. Mat. Palermo* **37** (1914) 371–375.

[12] Y. Jiang and A. Arabyan, A new pipe element for modeling three-dimensional large deformation problems. *Finite Elem. Anal. Des.* **22** (1996) 59–68.

[13] R. Kreb, On general hermite trigonometric interpolation. *Numer. Math.* **20** (1972) 125–138.

[14] A. Laulusa, O. Bauchau, J.-Y. Choi, V. Tan and L. Li, Evaluation of some shear deformable shell elements. *Int. J. Solids Struct.* **43** (2006) 5033–5054.

[15] C. Militello and A. Huespe, A displacement-based pipe elbow element. *Comput. Struct.* **29** (1988) 339–343.

[16] A. Prakash and K.D. Hjelmstad, A FETI-based multi-time-step coupling method for newmark schemes in structural dynamics. *Int. J. Numer. Methods Eng.* **61** (2004) 2183–2204.

[17] A.M. Yan, R.J. Jospin and D.H. Nguyen, An enhanced pipe elbow element: application in plastic limit analysis of pipe structures. *Int. J. Numer. Methods Eng.* **46** (1999) 409–431.

[18] E. Zafati, Convergence results of a heterogeneous asynchronous newmark time integrators. *ESAIM:M2AN* (2022).

[19] L. Zeng, L.G. Jansson and Y. Venev, On pipe elbow elements in ABAQUS and benchmark tests. In Vol. 3 *Design and Analysis*. American Society of Mechanical Engineers (2014).

[20] W.P. Ziemer, Weakly Differentiable Functions. Springer, New York (1989).

[21] A. Zygmund and R. Fefferman, Trigonometric Series. Cambridge University Press (2003).